Cytogenetic Prognostication within Medulloblastoma Subgroups

Shih, et al

Appendix

Cytogenetic Prognostication within Medulloblastoma Subgroups

The Medulloblastoma Advanced Genomics International Consortium (MAGIC)

List of Appendix Figures

List of Appendix Tables

Appendix Figure Legends

Appendix Fig A1. Overall survival curves for clinical prognostic markers and molecular subgroups. Kaplan-Meier curves depict survival of medulloblastoma patients, split by gender (A), age group (B), metastatic status (C), histology (D), and molecular subgroup (E).
Numbers below x-axis represent patients at risk of event; statistical significances are evaluated by log-rank tests; hazard ratio estimates (HR) are derived from Cox proportional-hazards analyses.

Appendix Fig A2. Overall survival curves for females and males within each medulloblastoma subgroup. Kaplan-Meier curves depict survival of females and males with each molecular subgroup of medulloblastoma, in the discovery cohort and the validation cohort.
Numbers below x-axis represent patients at risk of event; statistical significances are evaluated by log-rank tests; hazard ratio estimates (HR) are derived from Cox proportional-hazards analyses.

Appendix Fig A3. Overall survival curves for histotypes within each medulloblastoma subgroup. Kaplan-Meier curves depict survival of patients with WNT, SHH, Group3, or Group4 medulloblastomas, split by histotype, in the discovery cohort and the validation cohort. All WNT medulloblastomas in the validation cohort exhibit classic histology.
Numbers below x-axis represent patients at risk of event; statistical significances are evaluated by log-rank tests; hazard ratio estimates (HR) are derived from Cox proportional-hazards analyses.

Appendix Fig A4. Overall survival curves for M1 medulloblastoma patients. Kaplan-Meier curves depict survival of patients with each molecular subgroup of medulloblastoma, split by metastatic stage, in the discovery cohort and the validation cohort.
Numbers below x-axis represent patients at risk of event; statistical significances are evaluated by log-rank tests; hazard ratio estimates (HR) are derived from Cox proportional-hazards analyses.

Appendix Fig A5. Areas under time-dependent ROC curves for multivariate of Cox models parameterized by clinical and subgroup variables. (A) Curves depict areas under ROC curves (AUCs) at each time point for multivariate Cox proportional-hazards models parameterized by only clinical biomarkers, only molecular subgroups, or both. (B) Curves depict time-dependent AUCs for univariate Cox models parameterized by each variable. (C) Curves depict decreases in AUCs upon removal of each variable from the fully-parameterized multivariate Cox model.

Appendix Fig A6. Comparison of the prognostic values of WNT status and chromosome 6 loss. (A) Overall survival curves depicting the prognostic impact of chr6 loss in WNT medulloblastoma and non-WNT medulloblastoma. (B) Confidence intervals (95%) of hazard ratio for WNT status and chr6 loss under a multivariate Cox model for all medulloblastoma

patients. (C) Areas under time-dependent ROC curves for Cox models parameterized by either chr6 loss or WNT status. (D) Areas under time-dependent ROC curves, averaged across time-points, for Cox models parameterized by either chr6 loss or WNT status.

Appendix Fig A7. Prognostically significant molecular biomarkers identified by pan-cohort analysis of medulloblastoma *in toto.* 'Subgroup-specific' biomarkers are prognostically significant in pan-cohort analysis, but their prognostic values are limited to one specific medulloblastoma subgroup. 'Subgroup-driven' biomarkers are prognostically significant in pan-cohort analysis, but its prognostic value is driven by its enrichment in a particular medulloblastoma subgroup; they have no prognostic significance in any molecular subgroup. Numbers below x-axis represent patients at risk of event; statistical significances are evaluated by log-rank tests; hazard ratio estimates (HR) are derived from Cox proportional-hazards analyses.

Appendix Fig A8. Prognostically significant molecular biomarkers in SHH medulloblastoma. Overall survival curves are shown for each biomarker. Numbers below x-axis represent patients at risk of event; statistical significances are evaluated by log-rank tests; hazard ratio estimates (HR) are derived from Cox proportional-hazards analyses.

Appendix Fig A9. Overall survival curves for patients harbouring amplification of *MYCN*, *GLI2*, or both. Kaplan-Meier curves depict survival of patients with SHH medulloblastoma or Group4 medulloblastoma, in the discovery cohort and the validation cohort. Patients are stratified by presence or absence of *MYCN* amplification. Patients are also stratified by *GLI2* amplification, *MYCN* amplification, or co-amplification. No Group4 medulloblastoma exhibit *GLI2* amplification.

Appendix Fig A10. Copy-number aberrations on chr14q in SHH medulloblastoma. Copy-number heatmap (Integrative Genome Browser) depicts copy-number aberrations on chr14q for SHH medulloblastoma samples. Horizontal tracks represent the copy-number profile of each sample, sorted by loss of chr14q. Copy-number data is unavailable for chr14p due to lack of probes therein on the Affymetrix SNP6 platform. Blue, loss; red, gain.

Appendix Fig A11. Effects of excluding M1 patients on the prognostic significance of molecular-clinical risk-stratification schemes. Overall survival curves are shown for SHH, Group3, or Group4 medulloblastoma patients stratified by the proposed risk-stratification schemes, either with M1 patients excluded from analysis or classified as metastasis positive.

Appendix Fig A12. Assessment of the contribution of covariates to the prognostic value of each molecular-clinical risk-stratification model. (A) Plots of the distribution of each covariate within each risk group, for SHH, Group3, and Group4 medulloblastomas. Associations between risk groups and covariates were tested by Fisher's exact tests. (B) Log-likelihoods of Cox proportional-hazards models built stepwise from the null model. During stepwise variable selection, each covariate was added before the risk-stratification groups. Increases in model log-

likelihood upon inclusion of risk-stratification groups represent prognostic values that could not be explained by each covariate alone. Stepwise increases in model log-likelihood were assessed by analyses of deviance tests.

Appendix Fig A13. Assessment of residual prognostic value of covariates beyond each molecular-clinical risk-stratification mode. Log-likelihoods of Cox proportional-hazards models built stepwise from the null model. During stepwise variable selection, covariates were added after the risk-stratification groups in order to assess their residual prognostic values. Stepwise increases in model log-likelihood were assessed by analyses of deviance tests.

Appendix Fig A14. Application of clinical-molecular risk-stratification schemes to each age group in the discovery cohort. Overall survival curves for WNT, Group3, and Group4 medulloblastomas, stratified using the proposed risk-stratification schemes, within patients of all ages, infants, children, or adults.

Appendix Fig A15. Application of clinical-molecular risk-stratification schemes to each age group in the validation cohort. Overall survival curves for WNT, Group3, and Group4 medulloblastomas, stratified using the proposed risk-stratification schemes, within patients of all ages, infants, children, or adults.

Appendix Fig A16. Areas under time-dependent ROC curves for risk groups stratified using only clinical or molecular markers, or both. Curves depict areas under ROC curves (AUCs) at each time point for survival estimates of each risk-stratification model. Risk-stratification schemes incorporating clinical variables only, molecular variables only, or both types of variables, are depicted in different colors. Additionally, risk-stratification models developed for each molecular subgroup were assessed on either patients belonging to the same subgroup or other subgroups.

Appendix Fig A17. Prognostically significant molecular biomarkers in Group3 medulloblastoma. Overall survival curves are shown for each biomarker. Numbers below x-axis represent patients at risk of event; statistical significances are evaluated by log-rank tests; hazard ratio estimates (HR) are derived from Cox proportional-hazards analyses.

Appendix Fig A18. Prognostically significant molecular biomarkers in Group4 medulloblastoma. Overall survival curves are shown for each biomarker. Numbers below x-axis represent patients at risk of event; statistical significances are evaluated by log-rank tests; hazard ratio estimates (HR) are derived from Cox proportional-hazards analyses.

Appendix Fig A19. Copy-number aberrations on chr11 in Group4 medulloblastoma. Copy-number heatmap (Integrative Genome Browser) depicts copy-number aberrations on chr11 for Group4 medulloblastoma samples. Horizontal tracks represent the copy-number profile of each sample, sorted by loss of chr14q. Copy-number data is unavailable for chr14p due to lack of probes therein on the Affymetrix SNP6 platform. Blue, loss; red, gain.

Appendix Fig A20 Summary of sample sizes in the discovery and the validation sets. Numbers represent sample sizes for each combination of variables. Total sample size within each box appears in bold. Sample sizes for the analyses of iso17q are shown as an example in the discovery set. Samples that harbor neither iso17q nor balanced chr17 are not shown explicitly in a box; they have broad gain or loss of chr17.

Appendix Fig A21 Risk stratification of medulloblastoma by molecular subgroup, clinical biomarkers, and cytogenetic biomarker.

Appendix Information

Construction and validation of risk stratification models

In order to identify novel and robust prognostic biomarkers, the present study examined a discovery set and a validation set of medulloblastoma cases. The discovery set consisted of cases with patient survival follow-up, whole-genome copy-number profiles, and varying degree of clinical details, including age, gender, metastatic status, and histological subtype. This set of cases was acquired from several hospitals and tumour banks around the globe. Therefore, the patients in the discovery set represent a heterogeneously treated group with diverse ethnic backgrounds. In contrast, the validation set consisted of medulloblastoma patients who were uniformly treated at a single institution in Moscow (Burdenko Hospital) using standardized treatment protocols of the German HIT study group[1].

All available clinical variables and molecular markers were tested for prognostic association in the discovery set. Several clinical variables, such as metastatic status and age group, were categorized in multiple different ways, due to disagreements in the literature and clinical practice across continents. Due to the large number of candidate markers tested, a rigorous selection procedure was applied in order to select a small number of candidates to be validated in the external validation set using fluorescence *in situ* hybridization (FISH), which is routinely performed in modern pathology laboratories within hospitals.

Accordingly, the clinical and molecular candidate biomarkers were assessed by three approaches. First, the candidates were assessed by a cross-validation method, in order to estimate the expected validation rate of the biomarker. That is, whether the biomarker will likely validate in an independent cohort. Second, the sample size required for further validation in a prospective study was estimated for each candidate. Prognostic markers with small effect size (i.e. hazard ratio) or with low frequency may need impractically large sizes and are thus clinically irrelevant. Third, the candidates were combined in multivariate Cox proportional-hazards models in order to assess whether the biomarkers have prognostic values independent of one another. Biomarkers were prioritized by high validation rates, reasonably small sample sizes, and/or prognostically

significance in multivariate models. The selected biomarkers were then used to construct the risk stratification models for each medulloblastoma subgroup.

The proposed risk stratification models represent promising candidates for future prospective trials. The constituent biomarkers were selected based on analyses within a heterogeneous discovery set, and are likely generalizable to different patient populations. For a specific treatment protocol within a specific patient population, there may be prognostic markers that have better prognostic value, particularly those that were not assessed in the present study due to scope. Notwithstanding these limitations, the proposed risk stratification models have been validated in an independent cohort, and can serve as the basis for the informed design of a future prospective trial.

Rare events

Some molecular biomarker candidates (e.g. *MYC* amplification, chr17 gain) have only been observed in a relative small number of patients (~10). Notwithstanding their infrequency in specific subgroups of medulloblastoma (a rare disease), their prognostic significances are supported by log-rank tests, likely due to their large 'effect size' (i.e. hazard ratio). Such biomarker candidates, however, have low expected validation rate from cross-validation and large estimated sample sizes from power analysis. On account of their potential therapeutic impact, these candidates were nonetheless included in the risk stratification models based on their independent prognostic significance under multivariate Cox models. Indeed, the candidates were ultimately validated to be *bona fide* prognostic biomarkers in the external validation set.

Log-rank tests vs. Cox proportional-hazards test

Appendix tables present results from log-rank tests and Cox proportional-hazards tests, which may yield considerably different p-values. As log-rank tests do not assume proportional hazards, their results were preferred over those of Cox proportional-hazards tests. Univariate Cox proportional-hazards analyses were performed to estimate hazard ratios and sample sizes required for prospective studies.

Isolated vs. non-isolated events

Isolated arm events occur in the absence of whole-chromosome event; non-isolated events may occur in the context of a whole-chromosome event. In the appendix tables, chr17q|G denotes the gain of chr17q or gain of chr17, whereas chr17Q|G denotes the gain of chr17q without concurrent gain of the whole chr17.

Isochromosome events

The analyses of isochromosomes (e.g. iso17q) differ between the main figures and the appendix tables. In the appendix tables, samples with iso17q were compared against samples without iso17q, irrespective of other cytogenetic aberrations on chr17. However, iso17q in Group4 medulloblastoma, albeit statistically significantly associated with poor survival in Group4 patients, have a low validation rate (Appendix Table 10), suggesting that its statistical association may be indirect. This statistical significance may be due to the inclusion of patients with tumors harboring chr17 gain in the reference group, since chr17 gain is associated with good prognosis (Figure 5A). Therefore, samples with iso17q were compared against samples with balanced chr17 and samples with broad gain or loss of chr17 were excluded from Figure 2G-H.

Appendix Methods

Patient information

All tissues and clinicopathological information were serially collected in accordance with institutional review boards from various contributing centers. In the discovery set, although precise treatment dates were often unavailable, at least 95% of the patients were treated within the past 15 years using modern treatment protocols, including surgical resection, whole-brain and spinal irradiation, and/or chemotherapy. Discovery set samples were collected between 2005 and 2013, with a focus on samples with available fresh-frozen material. Among the samples with treatment details, the earliest diagnosis is July 1997 and the latest is August 2012. Samples in the validation set were all obtained from the Burdenko institute with no selection criterion applied. All patients in the validation set were treated between 1995 and 2010 according to standardized therapy protocols of the German HIT study group.[1]

Prognostic biomarker identification

During the identification of cytogenetic events and copy-number aberrations in the discovery set, all chromosomal events (or chromosome arm events) were compared against reference samples with balanced copy-number for the chromosome (or chromosome arm); samples with copy-number changes in the opposite direction were specifically excluded from each comparison. Subsequent to biomarker discovery, cross-validation was performed to estimate the reproducibility and generalizability of the potential biomarkers in an independent cohort. During cross-validation, the discovery set was split randomly into two subsets. First, the biomarkers are tested by the log-rank test on the first subset. Then, statistically significant biomarkers ($p < 0.05$) are tested again by the log-rank test on the second subset, with correction for multiple hypotheses testing. This process was repeated 10,000 times to estimate the expected validation rate of each biomarker. The number of times a biomarker is significant in the first subset is tallied as "# discovered" and the number of times a discovered biomarker is also significant in the second subset is tallied as "# cross-validated". The expected validation rate of each biomarker, calculated by the quotient: (# discovered) / (# cross-validated). The final set of biomarkers was further validated in the external validation set.

Multiple hypothesis testing correction

Within each biomarker identification analysis, correction for multiple hypothesis testing was performed by the Benjamini-Hochberg method during the cross-validation procedure. The analyses were conducted independently (and hence corrected independently) as follows:

1. Clinical biomarker identification across medulloblastoma
   (summarized in Appendix Table 5, "Cross-validation" worksheet)

2. Clinical biomarker identification within WNT medulloblastoma (summarized in Appendix Table 5, “Cross-valid” worksheet)
3. Clinical biomarker identification within SHH medulloblastoma (summarized in Appendix Table 5, “Cross-valid” worksheet)
4. Clinical biomarker identification within Group3 medulloblastoma (summarized in Appendix Table 5, “Cross-valid” worksheet)
5. Clinical biomarker identification within Group4 medulloblastoma (summarized in Appendix Table 5, “Cross-valid” worksheet)
6. Molecular biomarker identification across medulloblastoma (summarized in Appendix Table 6, “Cross-valid” worksheet)
7. Molecular biomarker identification within WNT medulloblastoma (summarized in Appendix Table 7, “Cross-valid” worksheet)
8. Molecular biomarker identification within SHH medulloblastoma (summarized in Appendix Table 8, “Cross-valid” worksheet)
9. Molecular biomarker identification within Group3 medulloblastoma (summarized in Appendix Table 9, “Cross-valid” worksheet)
10. Molecular biomarker identification within Group4 medulloblastoma (summarized in Appendix Table 10, “Cross-valid” worksheet)

Statistical analysis

The patient survival characteristics were right-censored at 5 years (or 10 years) and analyzed by the Kaplan-Meier method. Univariate comparison of two or more survival curves were performed using log-rank tests and the Cox proportional-hazards (PH) regression models. The predictive values of biomarkers were assessed by analyses of deviance tests under multivariate Cox models and by time-dependent receiver operating characteristic (ROC) analyses. Associations between covariates and risk groups were tested by the Fisher’s exact test. All statistical analyses were performed in the R software environment (v2.15), using R packages survival (v2.36), risksetROC (v1.0.4), powerSurvEpi (v0.0.6), and ggplot2 (v0.9.3).

Time-dependent ROC analysis

Time-dependent ROC analyses were performed using the CoxWeights function provided in the risksetROC (v1.0.4) R package. This function calculates areas under time-dependent ROC curves as described in Heagerty and Zheng.[2] AUC estimates of the fitted multivariate Cox models being assessed were calculated every month, from 1 month to 60 months, in order to determine the collective predictive performance of the biomarkers in the Cox models. Differences in AUC estimates among Cox models across time points were tested by Friedman rank sum tests.

Risk stratification model selection

Biomarkers identified in univariate survival analyses were tested by multivariate Cox PH models. All discovered biomarkers were tested for inclusion in the risk stratification model by multiple unbiased procedures: stepwise regression using forward selection, backward elimination and bidirectional elimination with the Akaike information criterion, as well as analyses of deviance tests.

Appendix References

1. Kortmann, R.D. et al. Postoperative neoadjuvant chemotherapy before radiotherapy as compared to immediate radiotherapy followed by maintenance chemotherapy in the treatment of medulloblastoma in childhood: results of the German prospective randomized trial HIT '91. *Int J Radiat Oncol Biol Phys* **46**, 269-79 (2000).
2. Heagerty, P.J. & Zheng, Y. Survival model predictive accuracy and ROC curves. *Biometrics* **61**, 92-105 (2005).

Appendix Figure A1 Shih, Northcott, Remke et al.

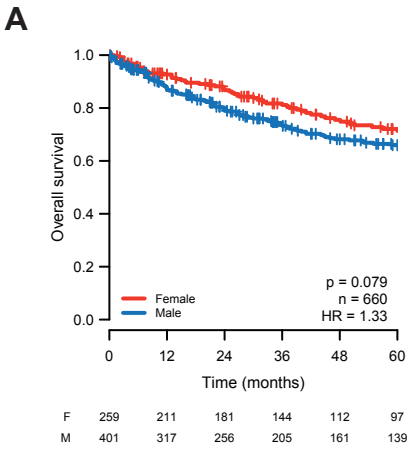

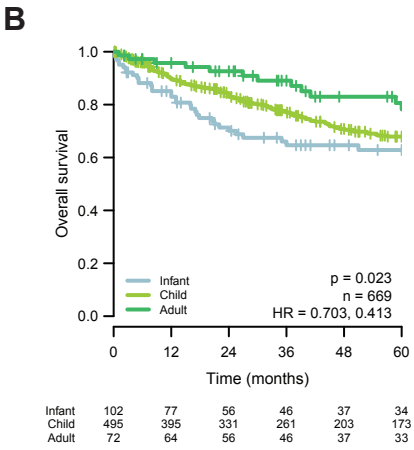

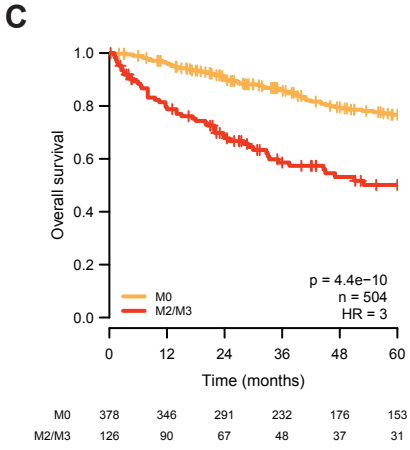

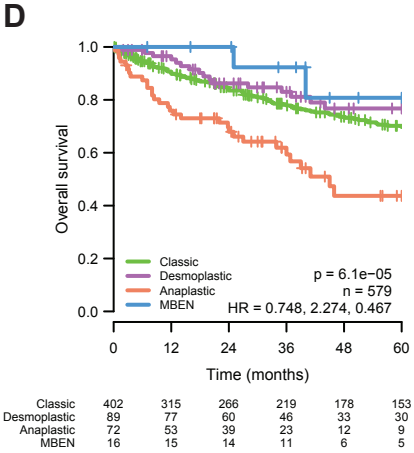

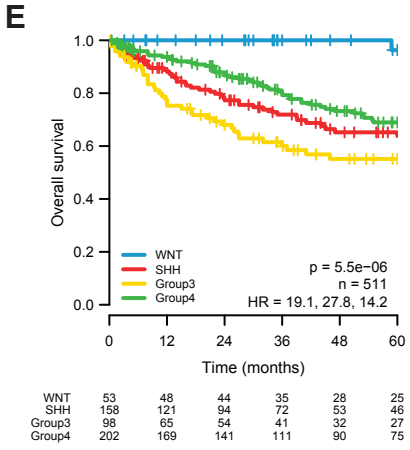

Appendix Figure A2 Shih, Northcott, Remke et al.

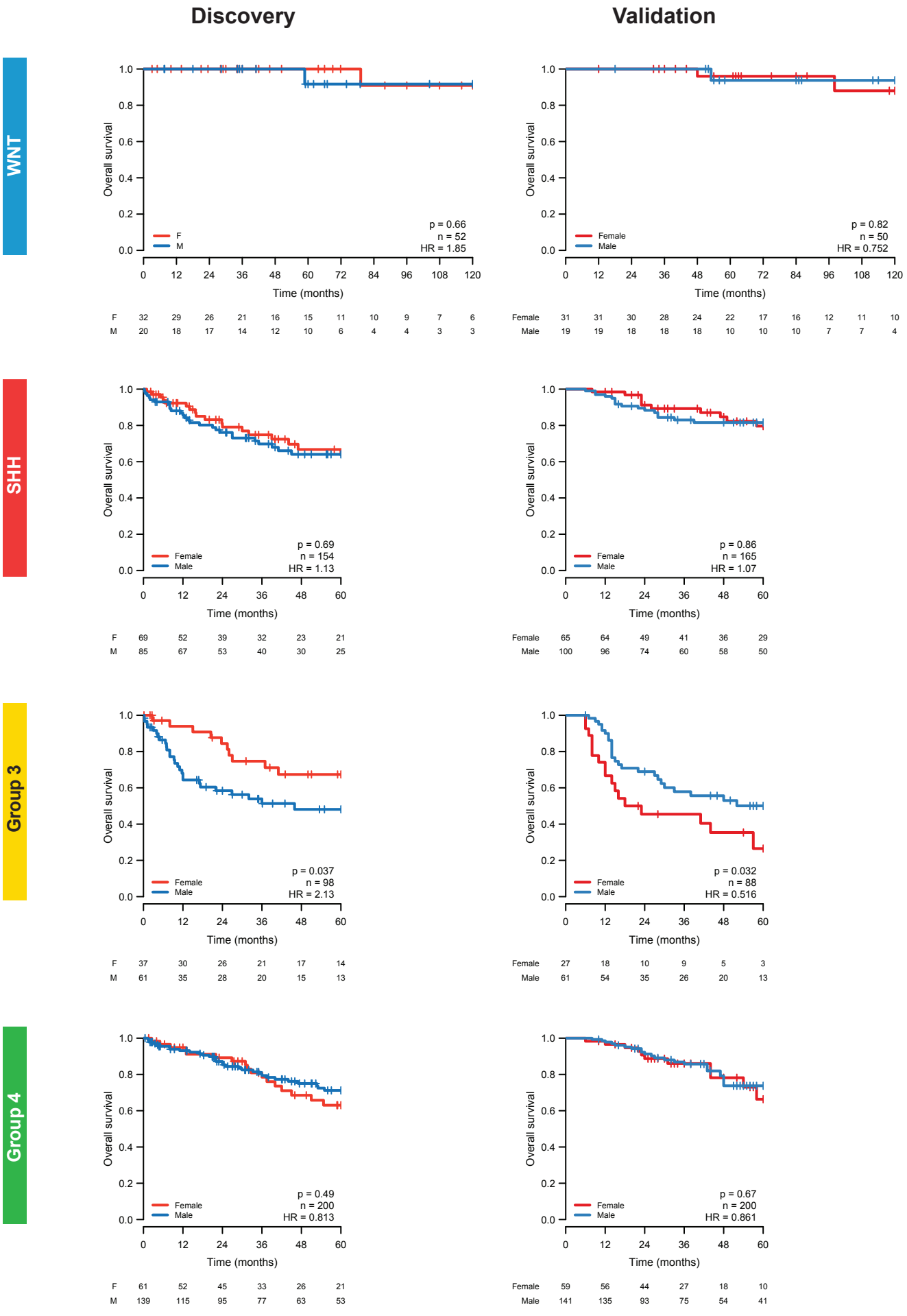

Appendix Figure A3 Shih, Northcott, Remke et al.

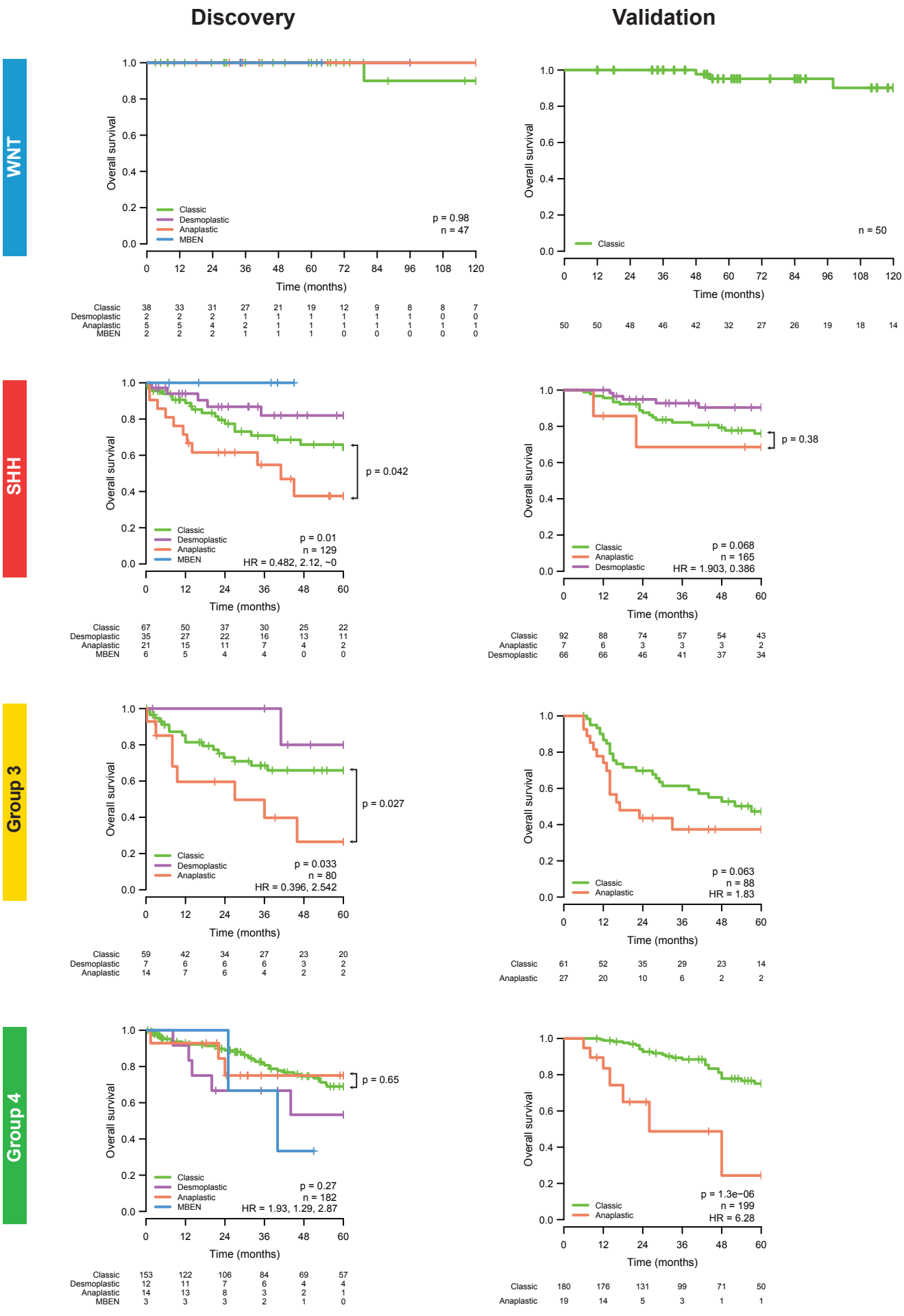

Appendix Figure A4 Shih, Northcott, Remke et al.

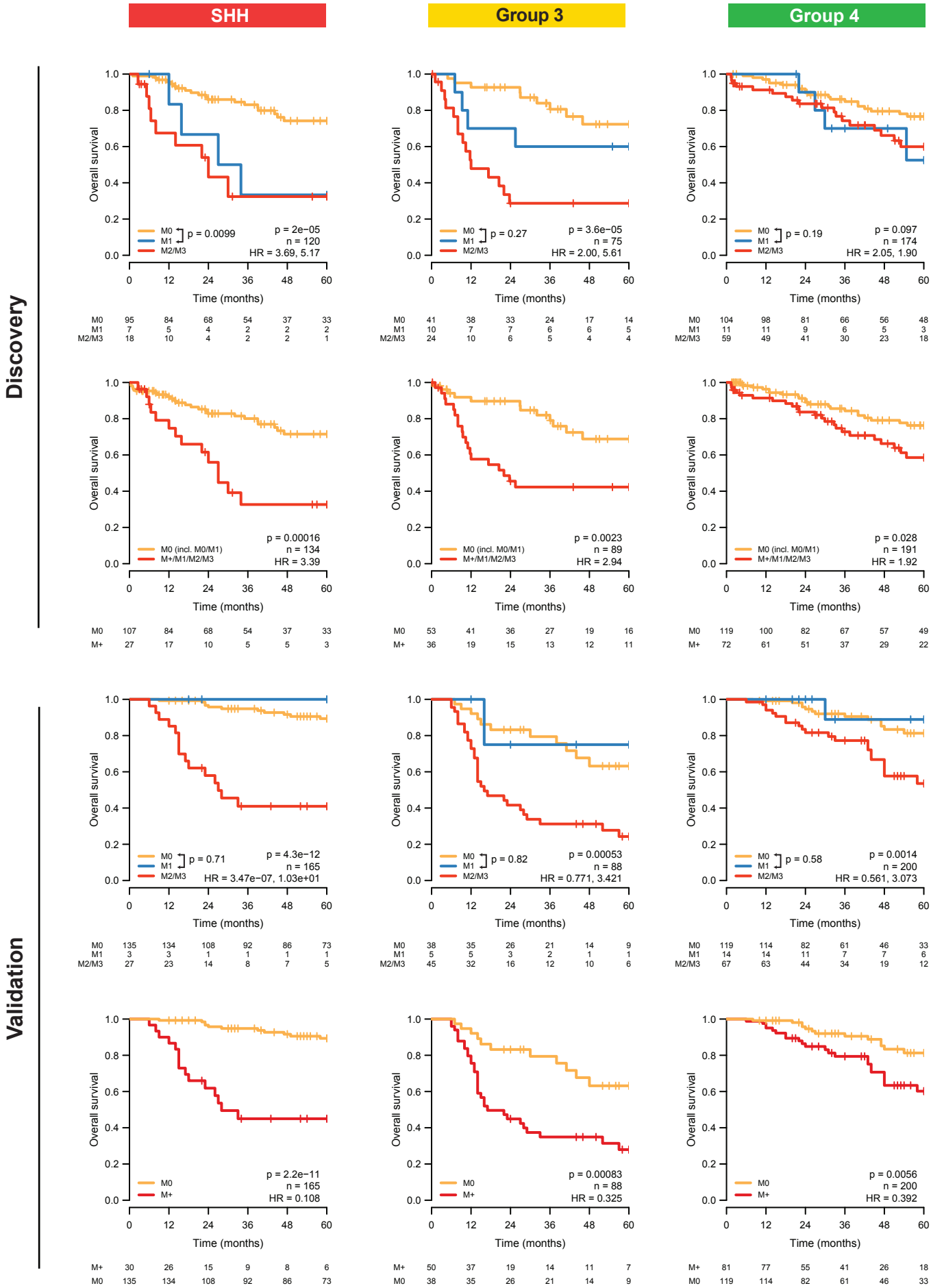

Appendix Figure A5 Shih, Northcott, Remke et al.

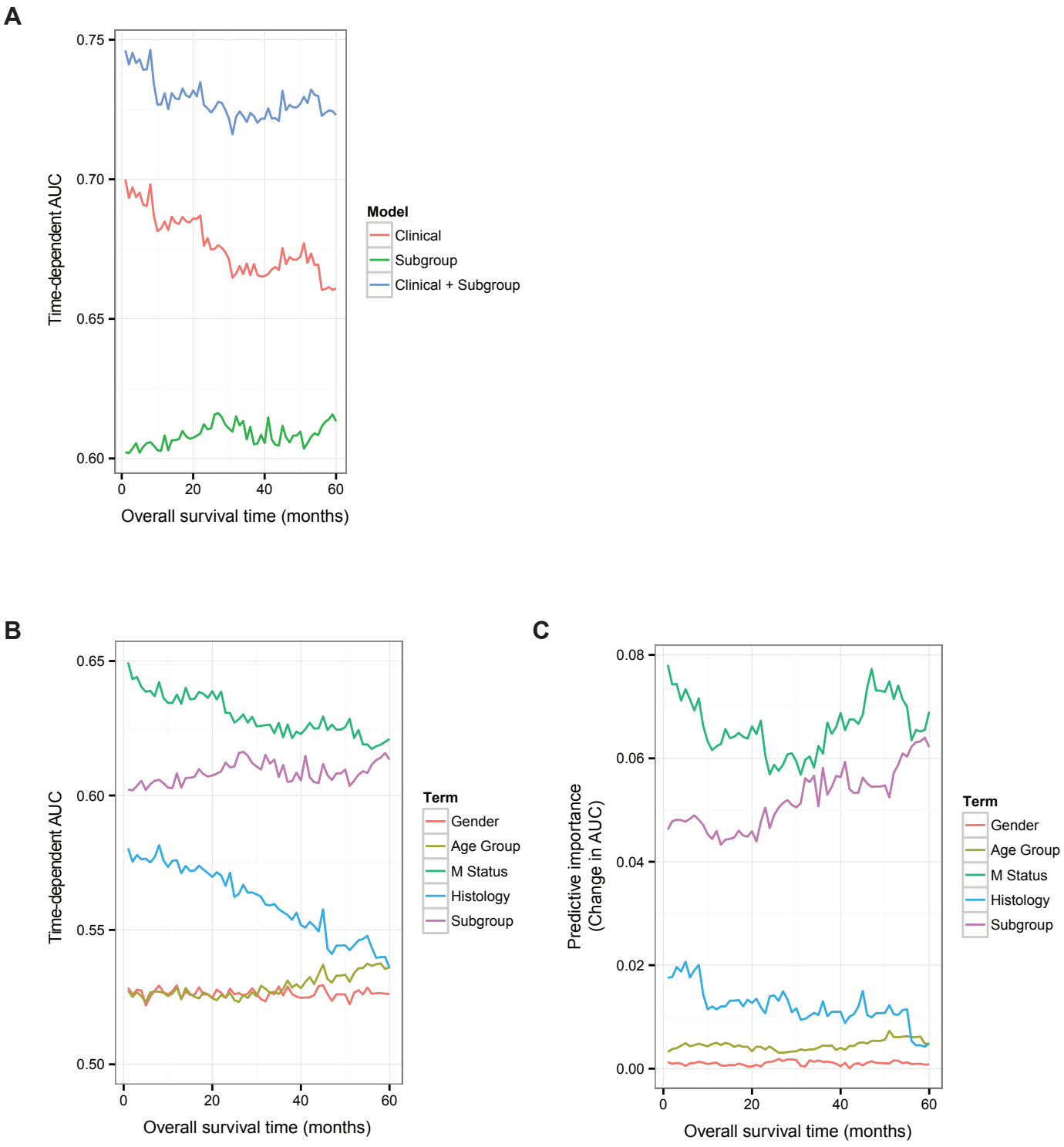

Appendix Figure A6 Shih, Northcott, Remke et al.

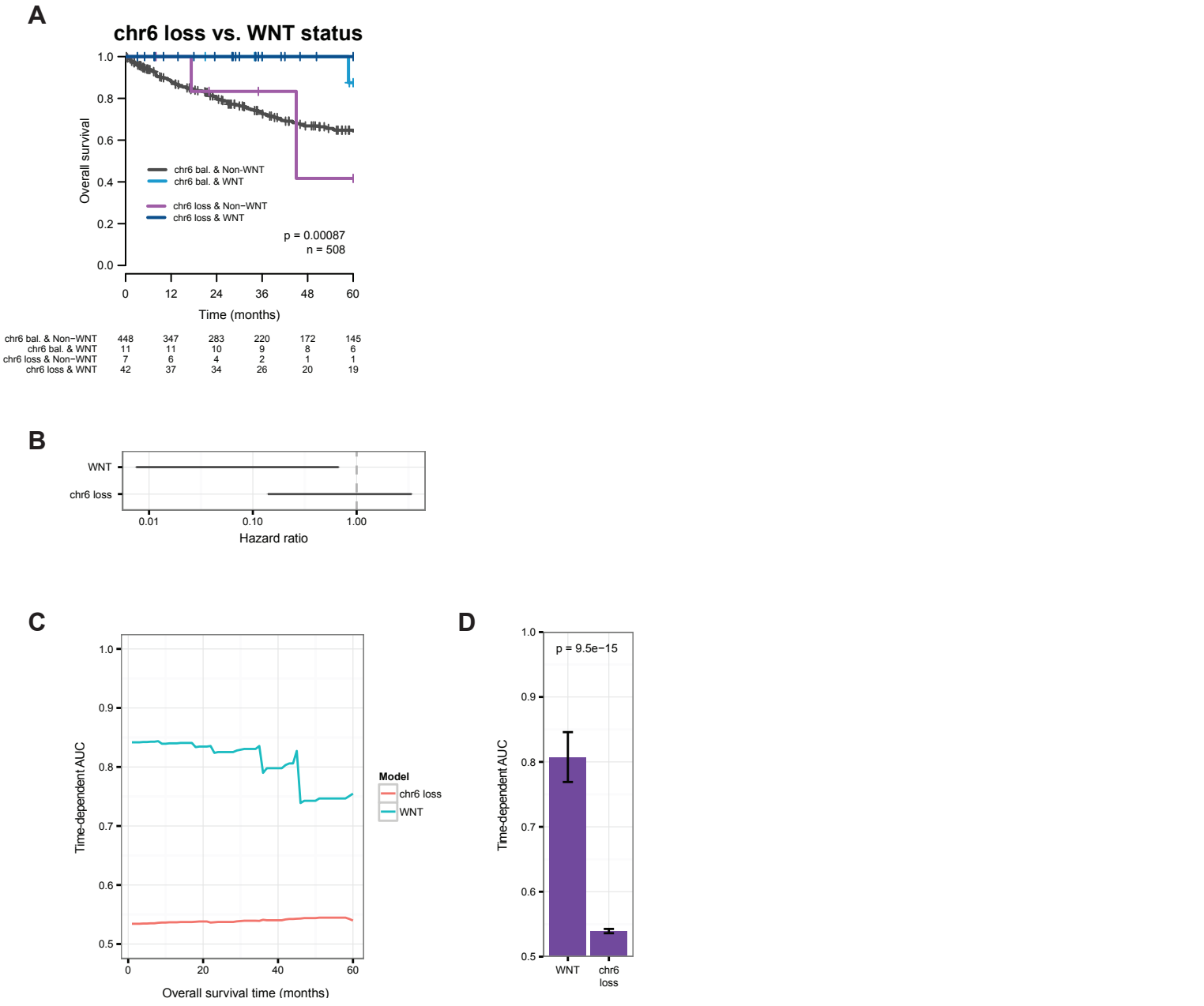

Appendix Figure A7 Shih, Northcott, Remke et al.

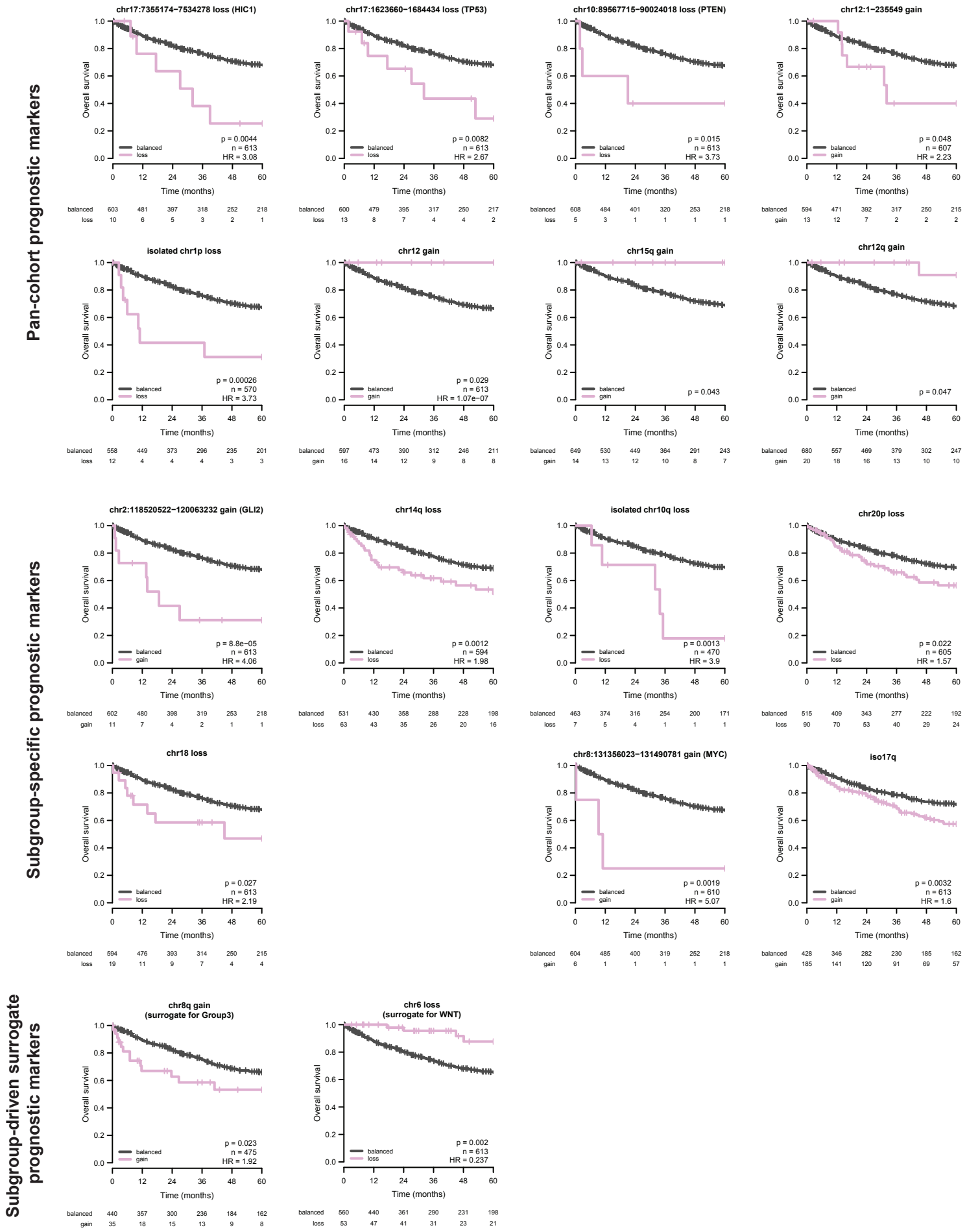

Appendix Figure A8 Shih, Northcott, Remke et al.

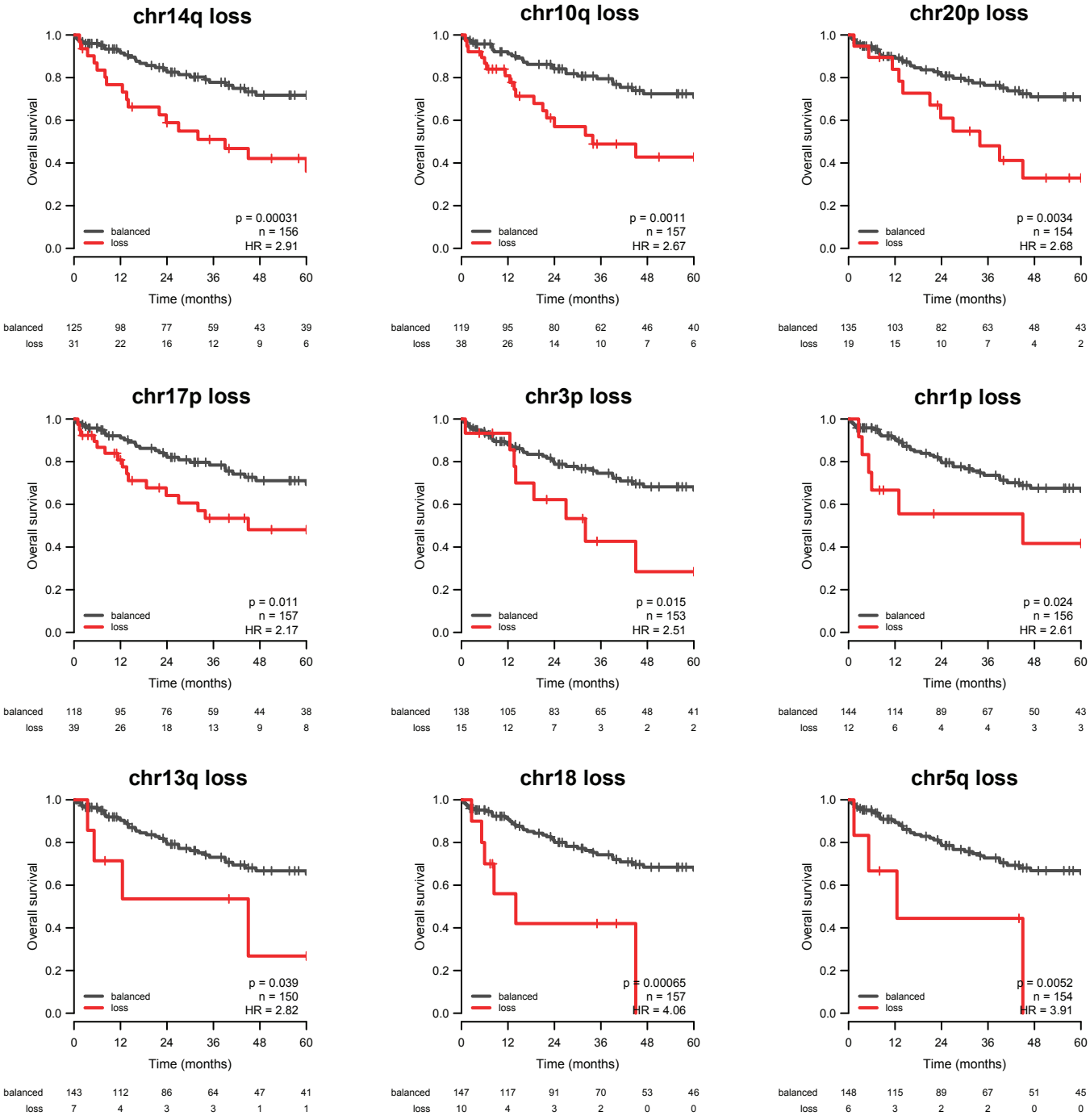

Appendix Figure A9 Shih, Northcott, Remke et al.

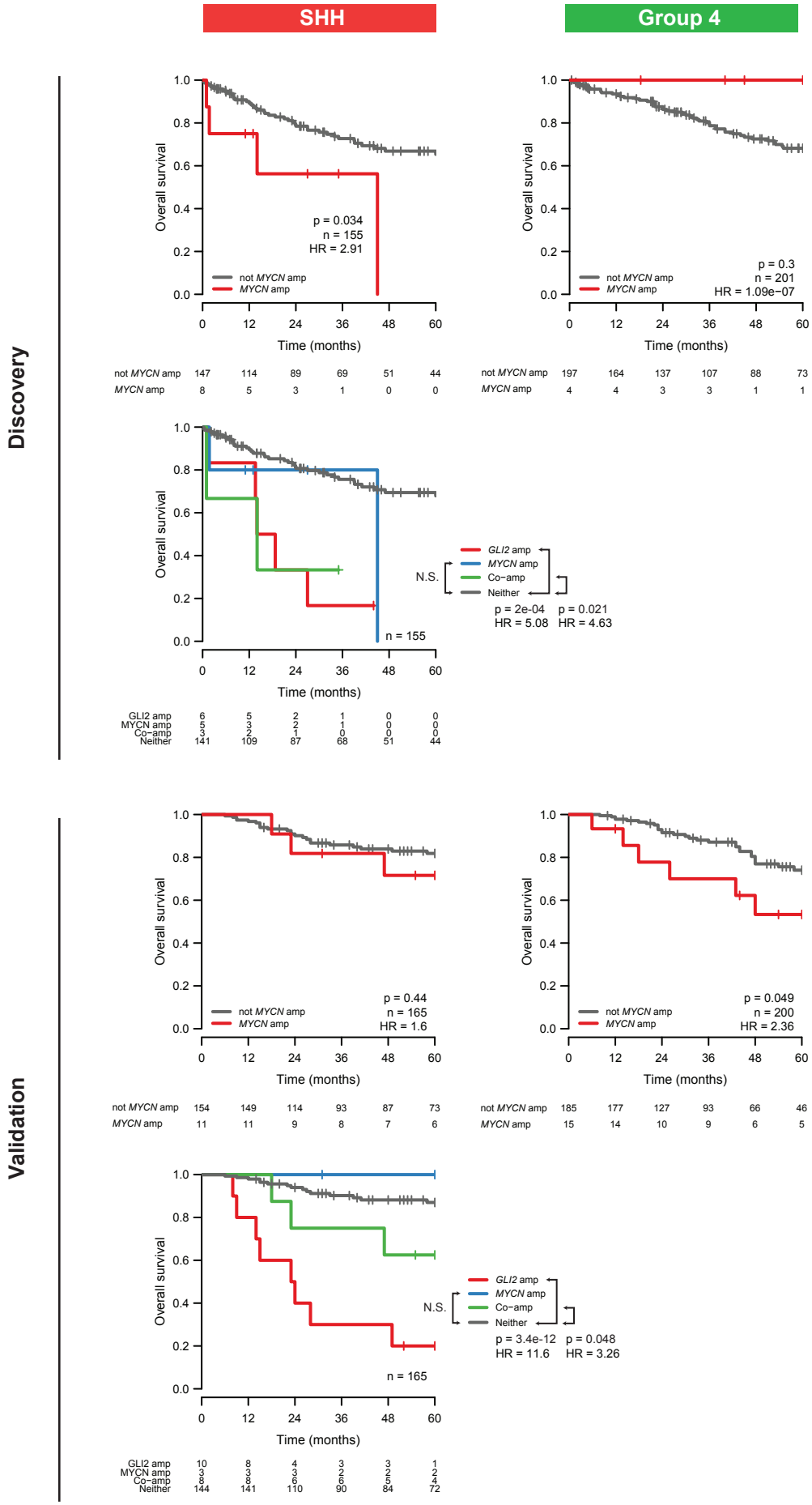

Appendix Figure A10 Shih, Northcott, Remke et al.

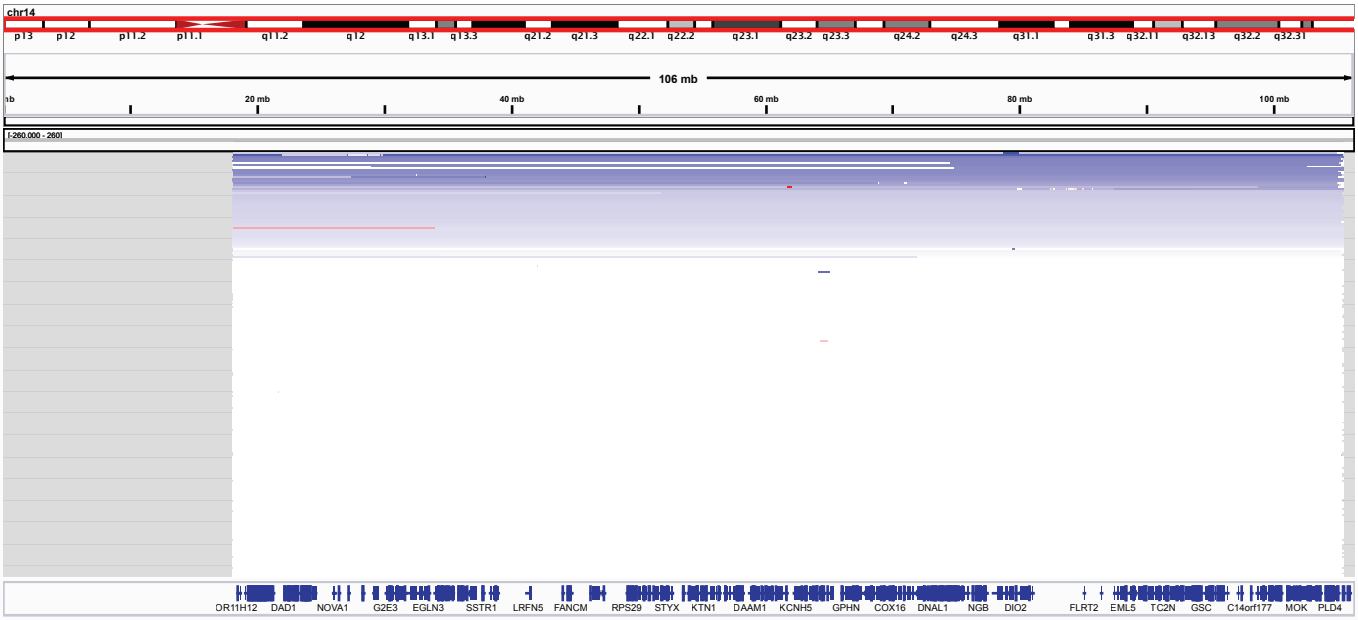

Appendix Figure A11 Shih, Northcott, Remke et al.

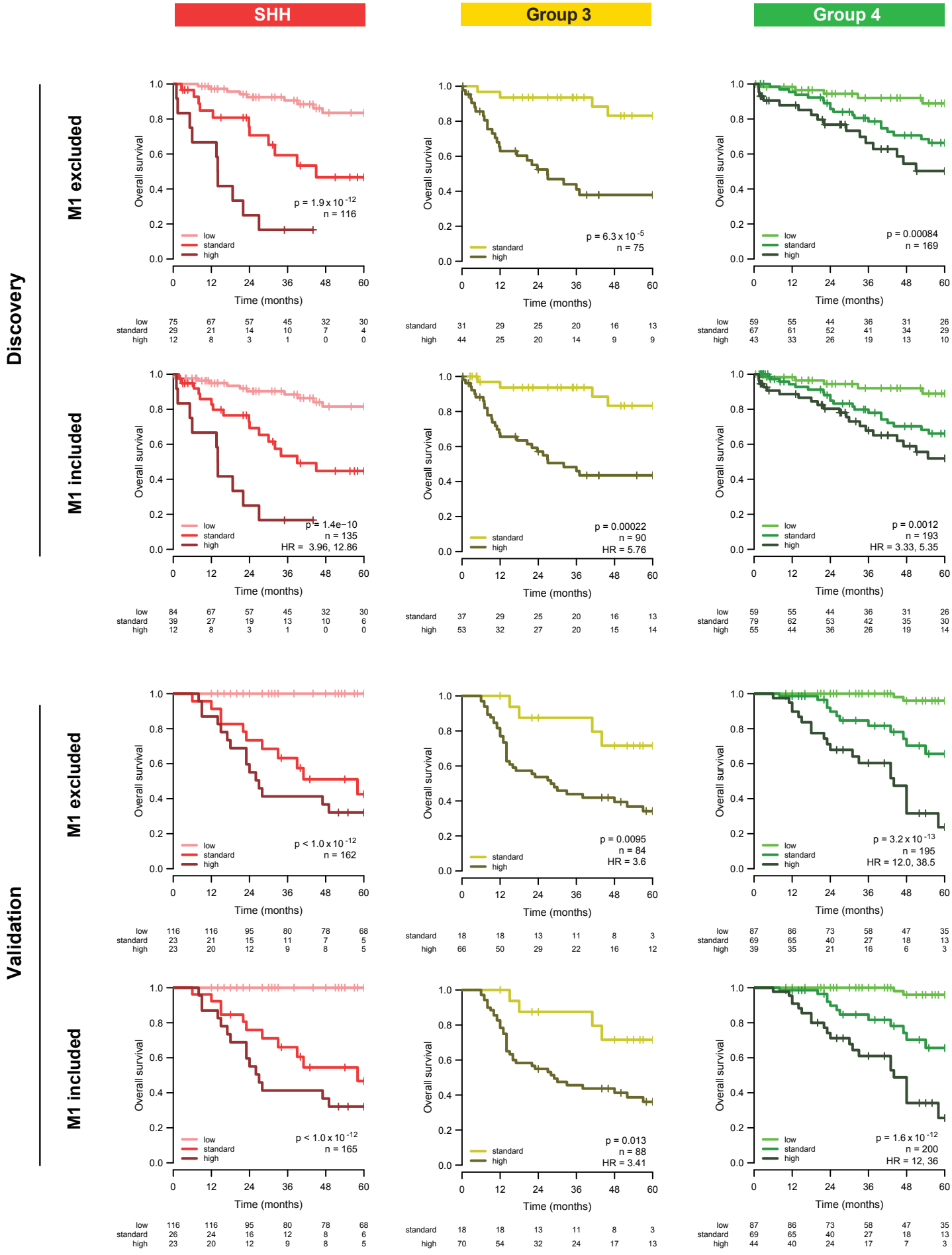

Appendix Figure A12 Shih, Northcott, Remke et al.

Appendix Figure A13 Shih, Northcott, Remke et al.

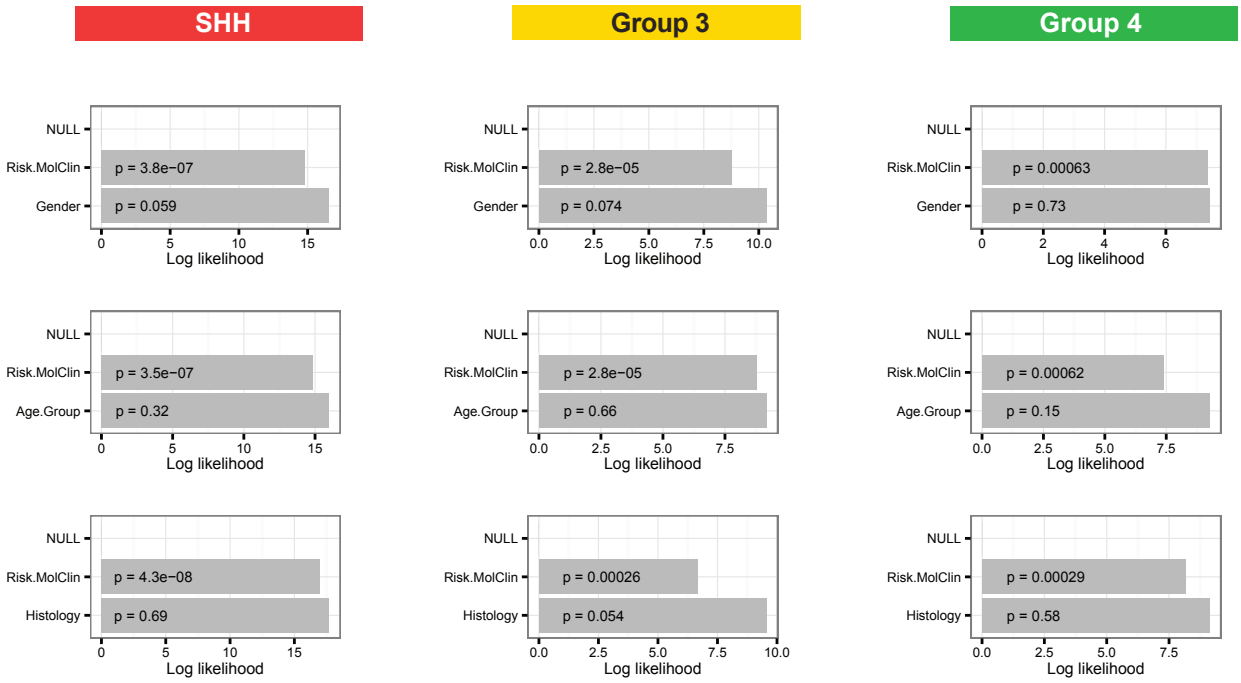

Appendix Figure A14 Shih, Northcott, Remke et al.

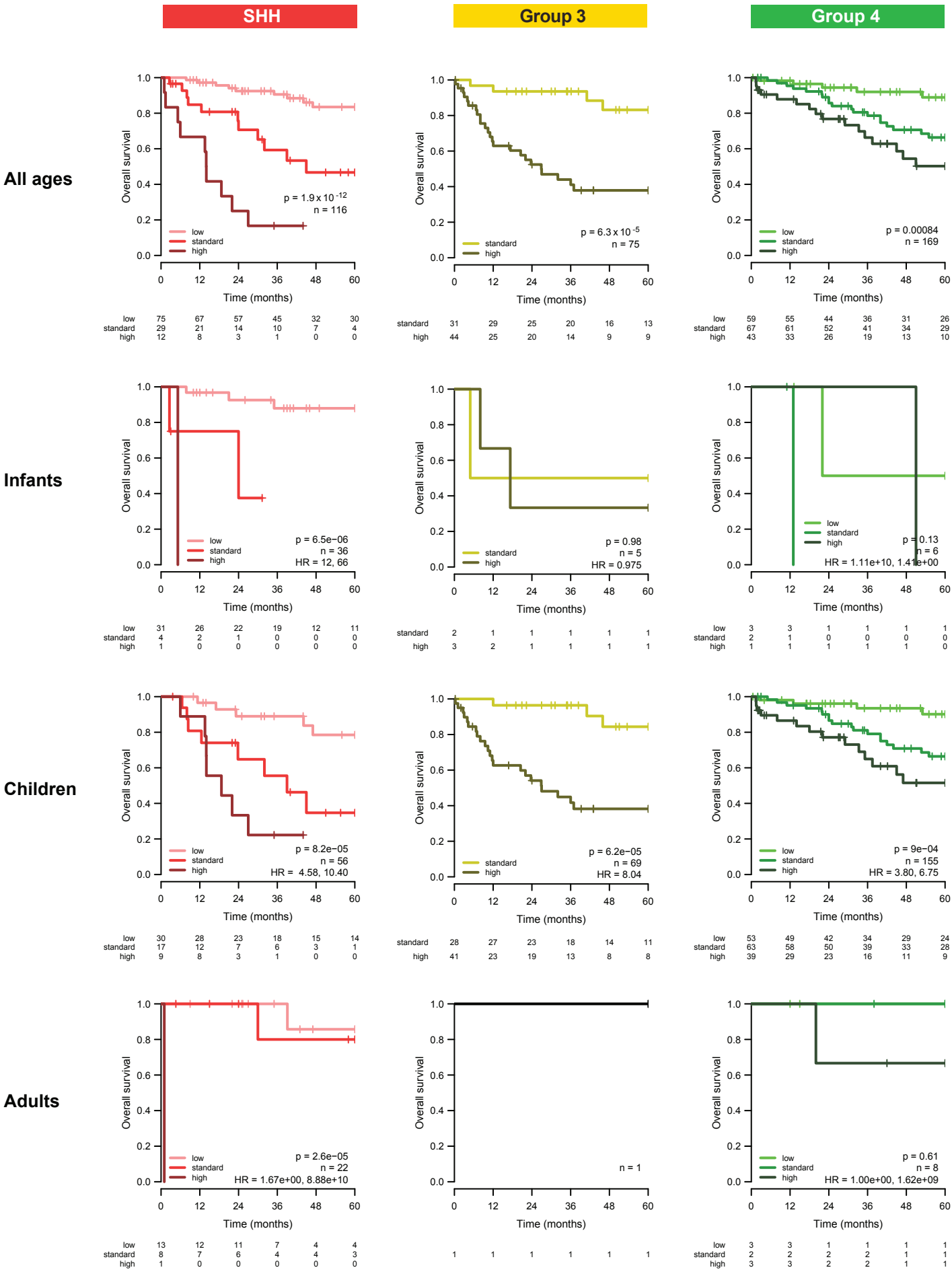

Appendix Figure A15 Shih, Northcott, Remke et al.

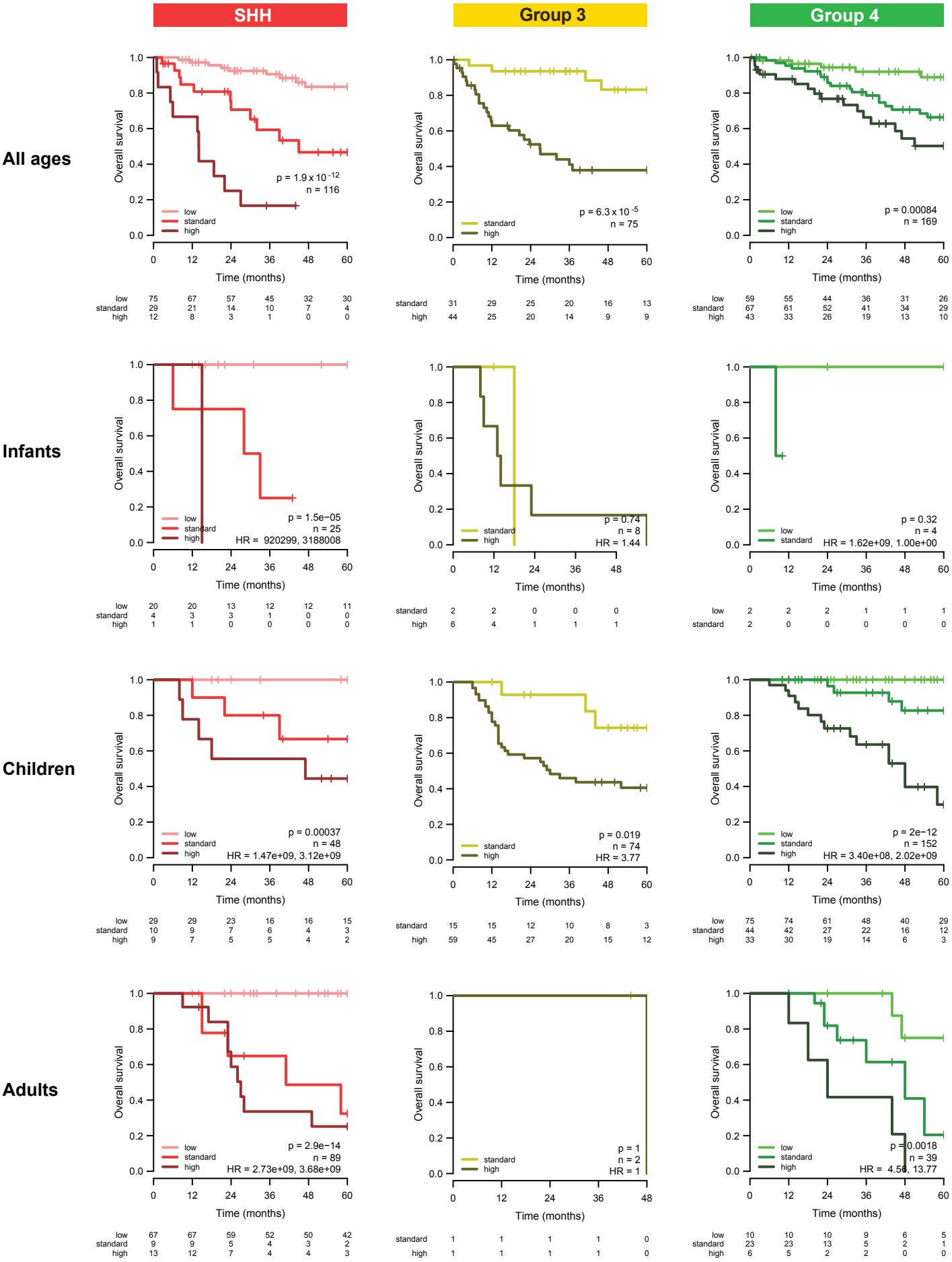

Appendix Figure A16 Shih, Northcott, Remke et al.

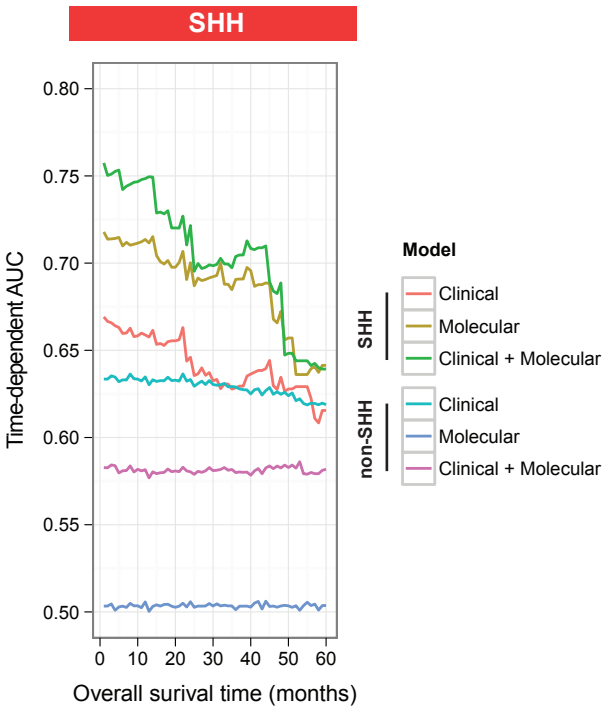

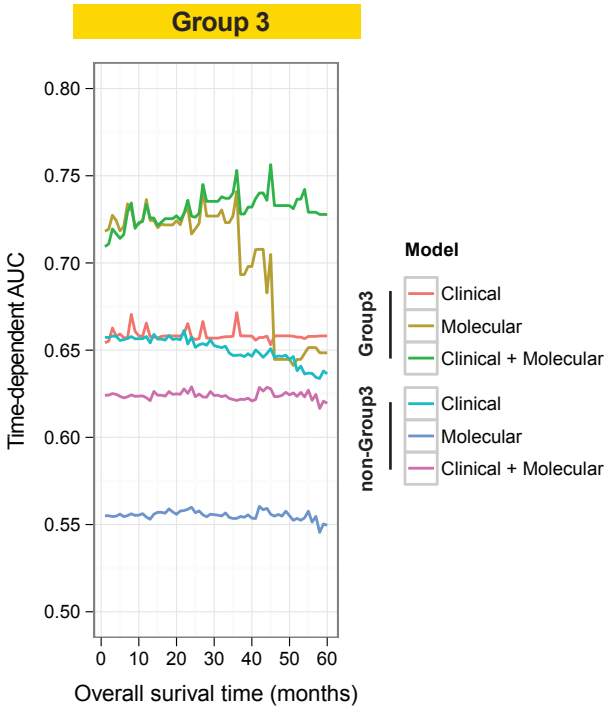

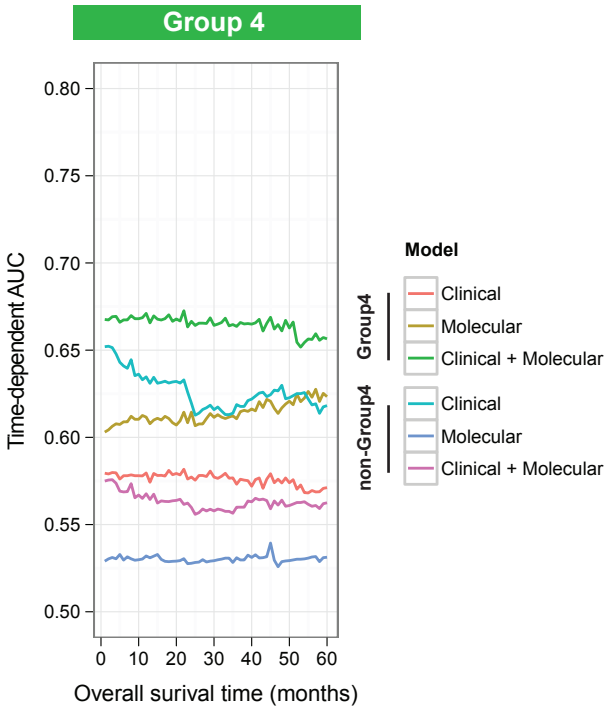

Appendix Figure A17 Shih, Northcott, Remke et al.

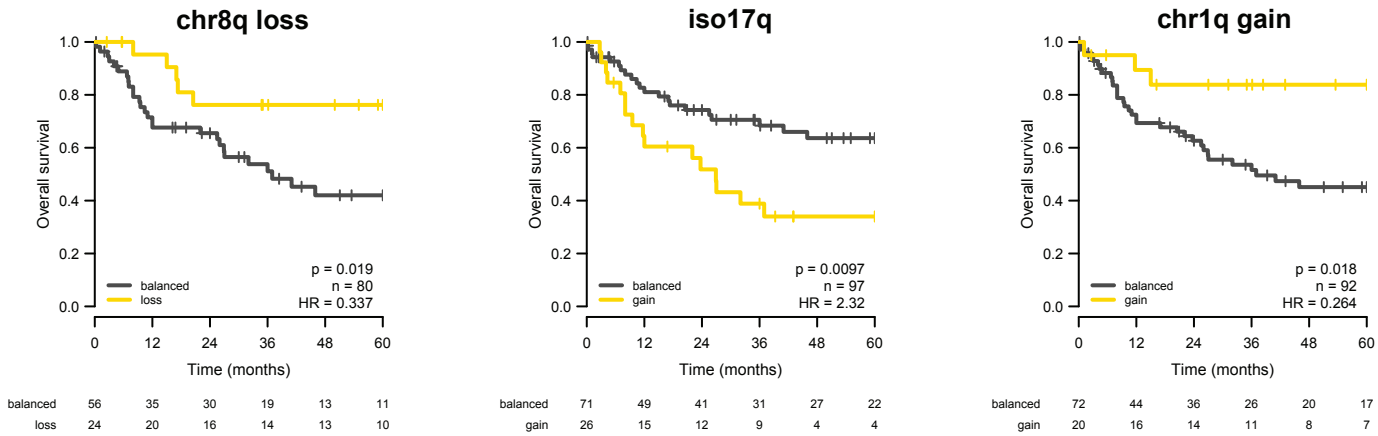

Appendix Figure A18 Shih, Northcott, Remke et al.

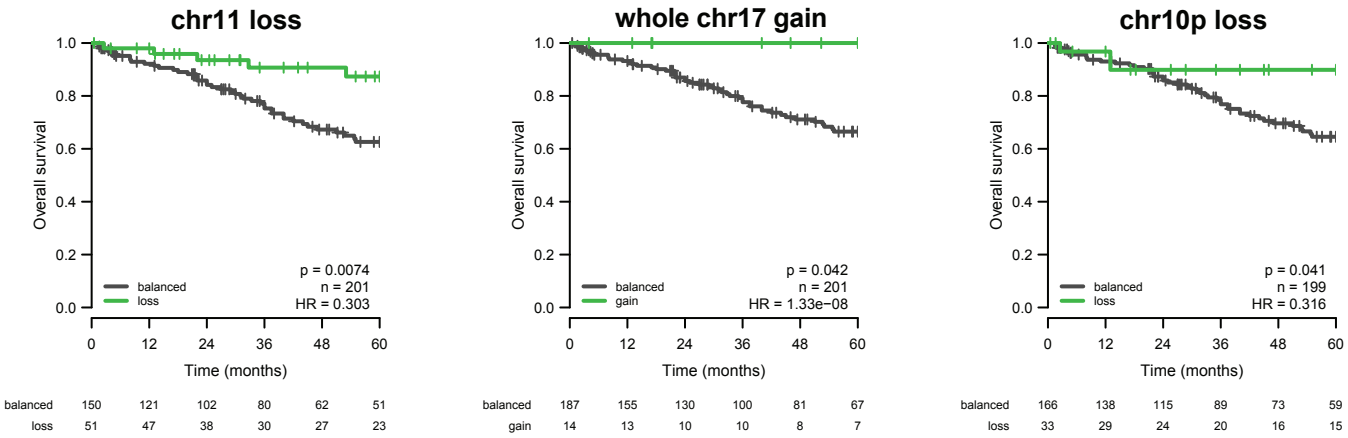

Appendix Figure A19 Shih, Northcott, Remke et al.

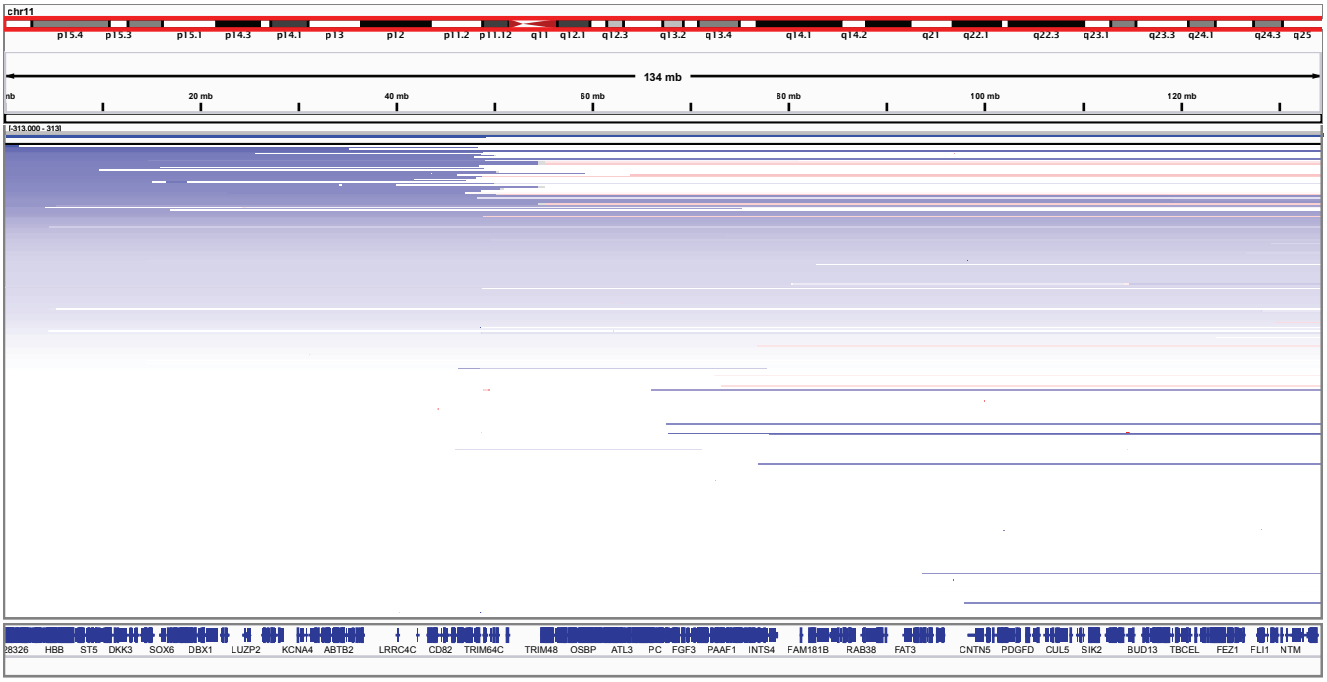

Appendix Figure A20 Shih, Northcott, Remke et al.

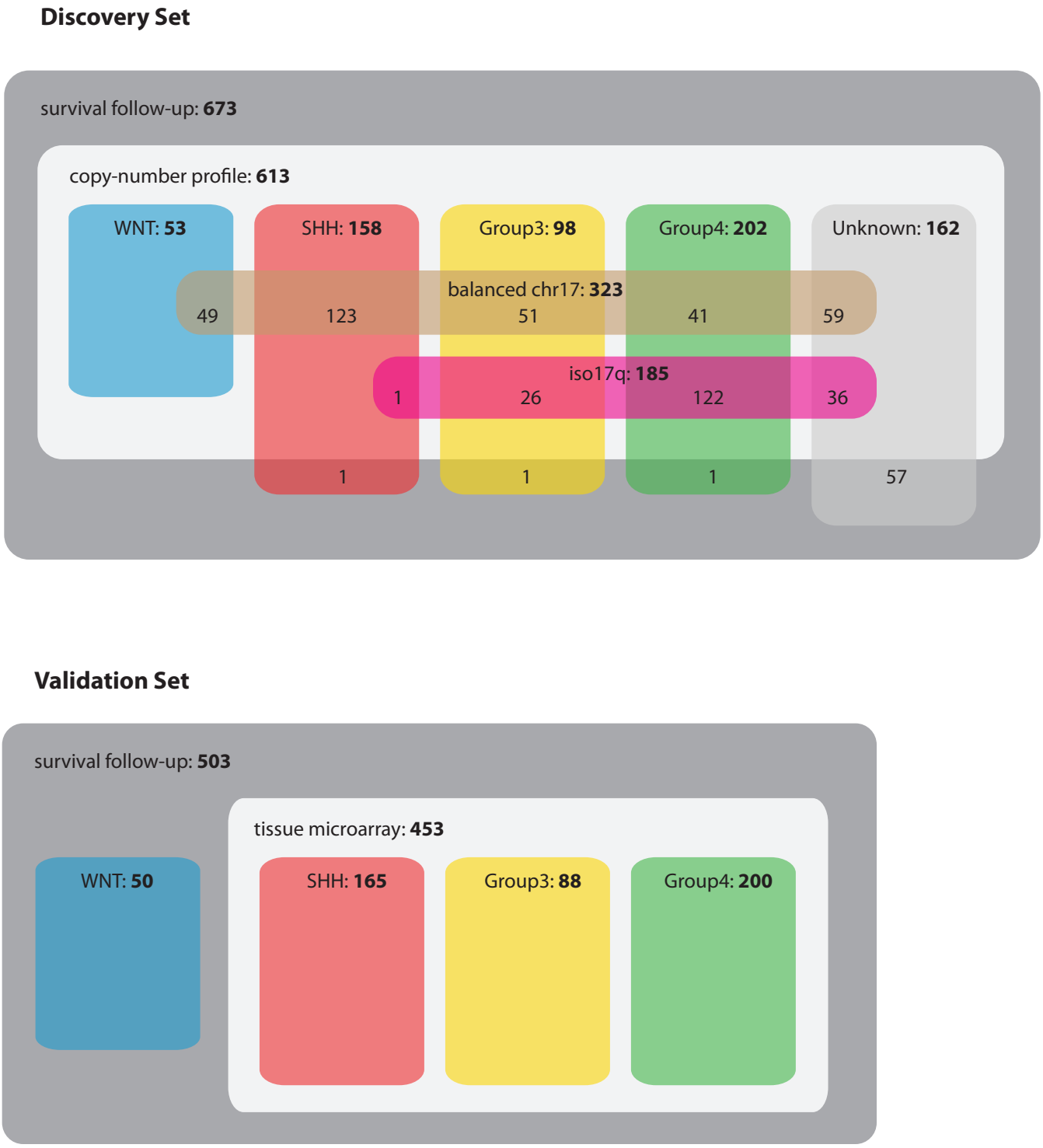

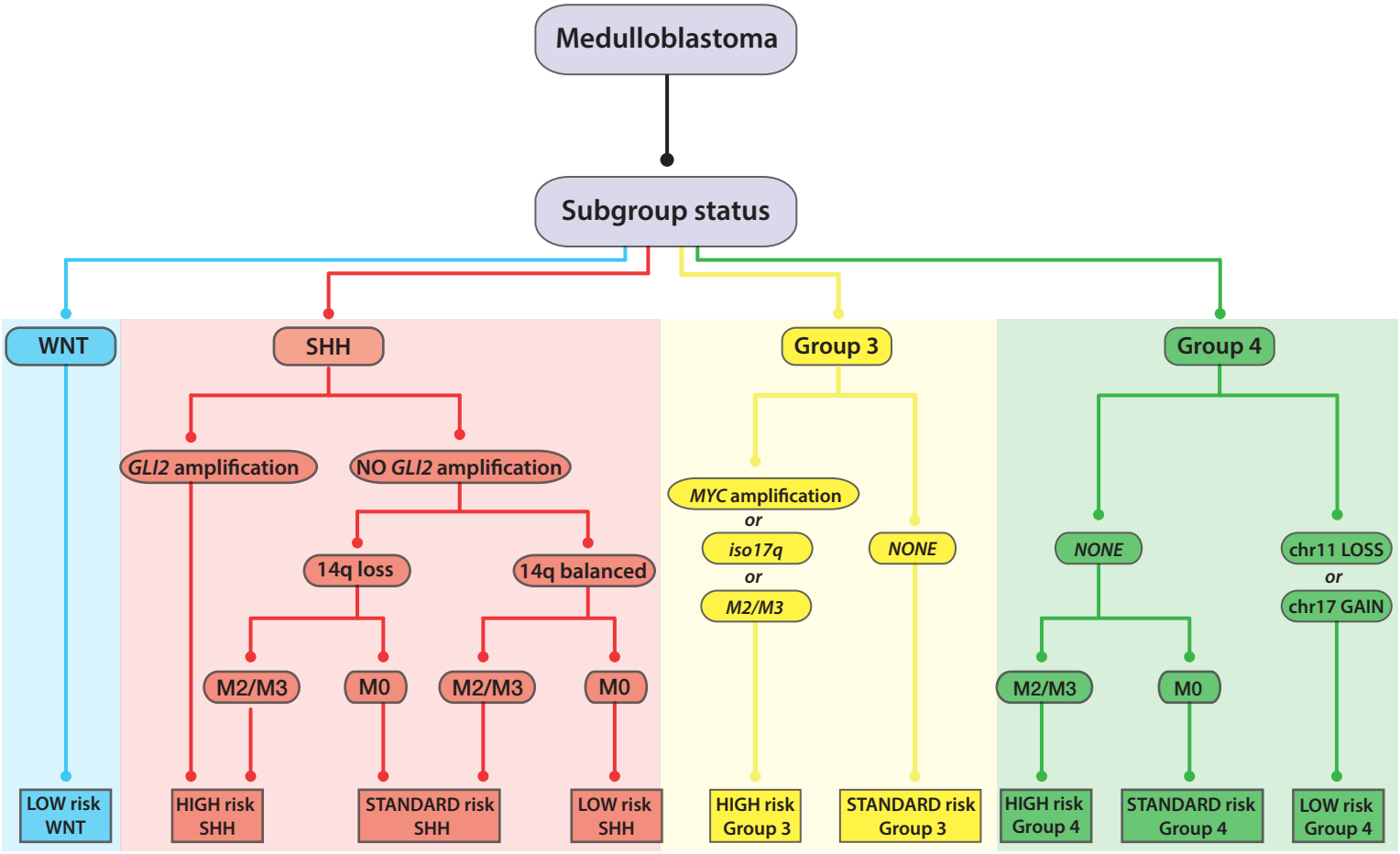
Medulloblastoma
Subgroup status
WNT
SHH
Group 3
Group 4
GLI2 amplification
NO GLI2 amplification
MYC amplification
or
iso17q
or
M2/M3
NONE
NONE
chr11 LOSS
or
chr17 GAIN
14q loss
14q balanced
M2/M3
M0
M2/M3
M0
M2/M3
M0
LOW risk WNT
HIGH risk SHH
STANDARD risk SHH
LOW risk SHH
HIGH risk Group 3
STANDARD risk Group 3
HIGH risk Group 4
STANDARD risk Group 4
LOW risk Group 4

Appendix Table A1. Patient characteristics of the discovery cohort (n = 673)

	WNT			SHH			Group3			Group4		
N (%)	53 (10.4)			158 (30.9)			98 (19.2)			202 (39.5)		
Age												
Median	9.5			6.5			5.3			8.5		
Range	2-56			0-47			1-17			1-36		
Group	Infant	Child	Adult	Infant	Child	Adult	Infant	Child	Adult	Infant	Child	Adult
N	1	42	9	49	72	35	11	85	2	9	180	13
%	1.9	80.8	17.3	31.4	46.2	22.4	11.2	86.7	2.0	4.5	89.1	6.4
Gender	Male	Female		Male	Female		Male	Female		Male	Female	
N	20	32		85	69		61	37		139	61	
Ratio (male : female)	0.62 : 1			1.23 : 1			1.65 : 1			2.27 : 1		
Metastatic status	M0	M1	M2/M3	M0	M1	M2/M3	M0	M1	M2/M3	M0	M1	M2/M3
N	41	2	3	95	7	18	41	10	24	104	11	59
%	89.1	4.3	6.5	79.2	5.8	15.0	54.7	13.3	32.0	59.8	6.3	33.9
Follow-up (months)†												
Median	59			51			62			75		
CI	36-72			41-70			43-70			55-82		
Survival (5-year) ‡												
%	96.3			63.8			55.1			69.0		
CI	89.4-100.0			55.5-73.4			45.1-67.4			61.8-76.9		

A total of 162 patients do not have subgroup affiliation.
Infant, age < 3; Child, 3 ≤ age < 16; Adult, age ≥ 16 years old.
M0, no metastasis; M1, presence in cerebrospinal fluid; M2/M3, macroscopic metastasis
CI, 95% confidence interval
† Schemper-Smith median follow-up time
‡ Kaplan-Meier survival time estimate

Appendix Table A2. Patient characteristics of the validation cohort (n = 453)

	SHH			Group3			Group4		
N (%)	165 (36.4)			88 (19.4)			200 (44.2)		
Age									
Median	17			5.0			9.0		
Range	0-59			1-29			2-50		
Group	Infant	Child	Adult	Infant	Child	Adult	Infant	Child	Adult
n	25	51	89	8	78	2	4	157	39
%	15.2	30.9	53.9	9.1	88.6	2.3	2.0	78.5	19.5
Gender	Male		Female	Male		Female	Male		Female
n	100		65	61		27	141		59
Ratio (male : female)	1.54 : 1			2.26 : 1			2.39 : 1		
Metastatic status	M0	M1	M2/M3	M0	M1	M2/M3	M0	M1	M2/M3
N	135	3	27	38	5	45	119	14	67
%	83.3	1.9	16.7	43.2	5.7	51.1	59.5	7.0	33.5
Follow-up (months)†									
Median	68			56			44		
CI	63-78			46-80			33-54		
Survival (5-year) ‡									
%	70.2			0.0			56.3		
CI	60.9-80.8						44.2-71.9		

Infant, age < 3; Child, 3 ≤ age < 16; Adult, age ≥ 16

M0, no metastasis; M1, presence in cerebrospinal fluid; M2/M3, macroscopic metastasis

CI, 95% confidence interval

† Schemper-Smith median follow-up time

‡ Kaplan-Meier survival time estimate

Appendix Table A3. Characteristics of WNT medulloblastomas

Sample	Age	Gender	Histology	M Stage	Status	**Exon 3 Mutation**		**Chromosome 6 Status**		
						Codon	Amino Acid	*p* arm	*q* arm	
MB-15	3	F	Classic	M0	ANED	GGA → GAA	G34E	loss	loss	
MB-18	8	M	Classic	M0	ANED	GAC → AAC	D32N	loss	loss	
MB-128	9	M	Classic	M1	Alive	GGA → GAA	G34E	loss	loss	
MB-145	10	M	Classic			GAC → TAC	D32Y	loss	loss	
MB-147	12	M	Classic			TCT → TGT	S33C	loss	loss	
MB-178	6	F	Classic	M0	ANED	GGA → AGA	G34R	loss	loss	
MB-190	36	M	Classic		ANED	GAC → TAC	D32Y	balanced	balanced	
MB-191	17	F	Classic		ANED	GGA → GAA	G34E	loss	loss	
MB-301	12	F	Classic	M1	Alive	GAC → AAC	D32N	loss	loss	
MB-302	8	F	Classic	M0	Alive	GAC → AAC	D32N	loss	loss	
MB-303	13	M	Classic	M0	Alive	TCT → CCT	S37P	loss	loss	
MB-307	12	M	Classic	M0	Alive	GAC → AAC	D32N	loss	loss	
MB-328	10	M	Classic	M0	Alive	TCT → TTT	S37F	loss	loss	
MB-336	8	M	Classic	M0	Alive	GGA → GAA	G34E	loss	loss	
MB-361	16	M	Classic	M0	Alive	GAC → GTC	D32V	loss	loss	
MB-401	8	M	Classic	M0	Alive	GAC → AAC	D32N	loss	loss	
MB-407	27	F	Classic	M0	Alive	TCT → TTT	S45F	balanced	balanced	
MB-408	27	M	Classic	M0	Alive	TCT → TAT	S37Y	balanced	balanced	
MB-416	19	F	Classic	M0	Alive	GAC → TAC	D32Y	loss	loss	
MB-418	18	F	Classic	M0	Alive	TCT → TGT	S33C	loss	loss	
MB-449	4	M				TCT → TGT	S37C	balanced	balanced	
MB-455	11	F	Classic	M0	ANED	GAC → TAC	D32Y	loss	loss	
MB-496	14	F	Classic	M0	Alive	GGA → AGA	G34R	loss	loss	
MB-498	6	F	Classic	M2	Alive	TCT → TGT	S33C	loss	loss	
MB-502	12	F	Classic	M0	Alive	GGA → AGA	G34R	loss	loss	
MB-505	12	F	Classic	M0	Alive	TCT → TGT	S33C	loss	loss	
MB-520	18.5	M		M0	DoD	TCT → TTT	S33F	balanced	balanced	
MB-521	56.32	M		M2	AWD	TCT → TGT	S33C	balanced	loss	
MB-662	9.4	F	Classic	M0/M1	ANED	GGA → GAA	G34E	loss	loss	
MB-670	10.4	M	Classic	M0/M1	ANED	GGA → GAA	G34E	loss	loss	
MB-695	11.81	M	Classic			TCT → TAT	S37Y	loss	loss	
MB-701	5.07	F	Classic			GAC → GGC	D32G	loss	loss	
MB-719	24.5	F	Classic	M0	ANED	TCT → TAT	S37Y	balanced	loss	

MB-788	12.91	F	Classic			TCT → TAT	S33Y	loss	loss	
MB-812	14.28	F	MBEN	M0	ANED	GGA → AGA	G34R	loss	loss	
MB-828	13	F		M0	ANED	GGA → AGA	G34R	loss	loss	
MB-873	9.83	M	Classic			TCT → TTT	S37F	loss	loss	
MB-883	7.76	M	Classic			GAC → AAC	D32N	loss	loss	
MB-891	16.57	M	Classic			TCT → TTT	S33F	loss	loss	
MB-905	8.84	F	Anaplastic			GAC → TAC	D32Y	loss	loss	
MB-956	5.62	M	Classic	M0	ANED	GAC → TAC	D32Y	loss	loss	
MB-972	12.24	F	Classic	M0	ANED	TCT → TTT	S33F	loss	loss	
MB-1055	15.95	F	Anaplastic			TCT → TTT	S33F	balanced	balanced	
MB-1082	9	F			Alive	GAC → TAC	D32Y	loss	loss	
MB-1089	5	F			Alive	TCT → TTT	S33F	balanced	balanced	
MB-1109	6	F	Classic	M0	ANED	GAC → GTC	D32V	loss	loss	
MB-1130	6	M	Anaplastic	M0	ANED	TCT → CCT	S33P	loss	loss	
MB-1169	8.18	F	Classic	M0	Alive	TCT → TGT	S37C	loss	loss	
MB-1171	8.3	F	Classic	M0	Alive	TCT → TTT	S37F	loss	loss	
MB-1198	7	M	Classic	M2	ANED	TCT → TGT	S33C	loss	loss	
MB-1235	20	F	Classic		ANED	TCT → TTT	S37F	balanced	balanced	
MB-1237						TCT → GCT	S37A	loss	loss	
MB-1255	2	F	Desmoplastic	M0	ANED	TCT → TGT	S33C	loss	loss	
MB-1259	16	F	Classic	M0	DoD	GAC → TAC	D32Y	balanced	loss	
MB-1275	8	F	Desmoplastic	M0	ANED	GAC → AAC	D32N	balanced	balanced	
MB-1299	12.6	M	Classic	M0	Alive	TCT → TGT	S33C	loss	loss	
MB-1321	6	F	Classic			GAC → AAC	D32N	balanced	balanced	
MB-1331	10	F	Classic	M3	AWD	GAC → TAC	D32Y	loss	loss	
MB-1335	8	M	Classic	M0	ANED	TCT → CCT	S33P	loss	loss	
MB-1343	10	M	Anaplastic	M0	ANED	TCT → TAT	S33Y	loss	loss	
MB-1355	10	F	Classic	M0	ANED	TCT → TGT	S33C	loss	loss	
MB-1368	8.1	F	Classic	M0	Alive	TCT → GCT	S33A	loss	loss	
MB-1380	9.33	M	Anaplastic	M0	AWD	GGA → AGA	G34R	loss	loss	
MB-389	11	M	Desmoplastic	M0	Alive	no mutation	no mutation	balanced	balanced	
MB-566	8	F	Classic	M0	ANED	no mutation	no mutation	balanced	balanced	
MB-687	4	M	Classic			no mutation	no mutation	loss	loss	
MB-811	15.3	M	Classic	M0	ANED	no mutation	no mutation	loss	loss	
MB-865	9.85	F	Classic			no mutation	no mutation	loss	loss	
MB-1026	7.44	F	Classic			no mutation	no mutation	balanced	balanced	
MB-1029	8.57	M	Classic			no mutation	no mutation	loss	loss	

MB-1220	12	M	Classic	M0	ANED	no mutation	no mutation	balanced	Balanced	

F, female; M, male;

MBEN, medulloblastoma with extensive nodularity;

M0, no metastasis;
M1, presence of tumor cells in the CSF;
M2, nodular seeding in the cerebellar or cerebral subarachnoid space or in the third or lateral ventricle;
M3, metastasis in spinal subarachnoid space;

ANED, alive no evidence of disease; AWD, alive with disease; DoD, died to disease

Appendix Table A4. Association analysis between molecular markers and metastasis	**Column1**
Worksheets	
Description	Description of worksheets.
WNT	Association analysis in WNT medulloblastoma
SHH	Association analysis in SHH medulloblastoma
Group3	Association analysis in Group3 medulloblastoma
Group4	Association analysis in Group4 medulloblastoma
Definitions	
Subgroup	Molecular subgroup of medulloblastoma, determined by a nanoString-based assay as previously described (Northcott et al. 2012. Acta Neuropathol, 123(4):615-26).
Metastasis	Staged according to Chang's metastasis staging system: M0 (no metastasis), M1 (presence of tumor cells in the CSF), M2 (nodular seeding in the cerebellar or cerebral subarachnoid space or in the third or lateral ventricle), M3 (metastasis in spinal subarachnoid space).
Association	Association between leptomeningeal dissemination (M1/M2/M3) and each molecular marker was tested using Fisher's exact test, with multiple hypothesis correction by the Benjamini-Hochberg method.

	Appendix Table A5. Analysis of candidate prognostic clinical markers for the discovery cohort
Worksheets	
Description	Description of worksheets.
Cross-validation	Cross-validation analyses of prognostically significant biomarkers.
Power	Sample size calculations under Cox proportional-hazards models of candidate prognostic biomarkers for prospective trials.
Definitions	
Survival	Patient overall survival, right-censored at 5 years after diagnosis.
Subgroup	Molecular subgroup of medulloblastoma, determined by a nanoString-based assay as previously described (Northcott et al. 2012. Acta Neuropathol, 123(4):615-26).
Metastasis	Staged according to Chang's metastasis staging system: M0 (no metastasis), M1 (presence of tumor cells in the CSF), M2 (nodular seeding in the cerebellar or cerebral subarachnoid space or in the third or lateral ventricle), M3 (metastasis in spinal subarachnoid space).
	M.Status1, M0 vs. M1/M2/M3; M.Status2, M0 vs. M2/M3; M.Status3, M0 vs. M1 vs. M2/M3
Age	Infant, age < 3; Child, 3 ≤ age < 16; Adult, age ≥ 16; Pediatric, age < 16
	Age.Group, Infant vs. Child vs. Adult; Age.Group2, Pediatric vs. Adult; Pediatric.Group, Infant vs. Child
Histology	Classic vs. Desmoplastic variants vs. Anaplastic variants vs. Medulloblastoma with Extensive Nodularity
Chromothripsis	Presence of at least one chromosome with ≥ 10 breakpoints.

Appendix Table A6. cohort	**Analysis of candidate prognostic molecular markers across all medulloblastoma for the discovery**
Worksheets	
Description	Description of worksheets.
Log-rank	Significance testing of overall survival differences between patients with or without biomarkers by the log-rank test.
Cross-validation	Cross-validation analyses of prognostically significant biomarkers.
Power	Sample size calculations under Cox proportional-hazards models of candidate prognostic biomarkers for prospective trials.
Definitions	
Survival	Patient overall survival, right-censored at 5 years after diagnosis.
Subgroup	Molecular subgroup of medulloblastoma, determined by a nanoString-based assay as previously described (Northcott et al. 2012. Acta Neuropathol, 123(4):615-26).
Event	DNA copy-number aberration (gain or loss) that spans at least an entire chromosome arm (broad), or a region that is < 12 Mbp in size (focal). G, gains; L, loss.
Identification	Broad and focal copy-number aberrations were identified by Affymetrix SNP6 copy-number profiling as previously described (Northcott et al. 2012. Nature, 488(7409):49-56).
Chromosome-arm	Distinction is made between two types of chromosome-arm events: isolated (P or Q) and non-isolated (p or q). Isolated arm events occur in the absence of whole-chromosome event; non-isolated events may occur in the context of a whole-chromosome event. For example, chr17q|G denotes the gain of chr17q or gain of chr17, whereas chr17Q|G denotes the gain of chr17q without concurrent gain of the whole chr17.
Comparison	For broad cytogenetic markers, the survival of patients whose tumours harbour gain or loss of the indicated chromosome arm were compared against those whose tumours have balanced copy-number for the said chromosome arm. For focal events, patients whose tumours harbour the events were compared against those whose tumours do not harbour the same focal event but may harbour broad events encompassing the locus.
Sample size	Sample sizes required to achieve 80% power in prospective trials are estimated based on the observed hazard ratio. Unbalanced design assumes that the proportion of test group subjects will be equal to the observed frequency of subjects wth the event in the discovery cohort. Balanced design assumes that the test and reference groups will be equal in size.

Appendix Table A7. Analysis of candidate prognostic molecular markers in WNT medulloblastoma for the discovery cohort	
Worksheets	
Description	Description of worksheets.
Log-rank	Significance testing of overall survival differences between patients with or without biomarkers by the log-rank test.
Cross-validation	Cross-validation analyses of prognostically significant biomarkers.
Power	Sample size calculations under Cox proportional-hazards models of candidate prognostic biomarkers for prospective trials.
Definitions	
Survival	Patient overall survival, right-censored at 5 years after diagnosis.
Subgroup	Molecular subgroup of medulloblastoma, determined by a nanoString-based assay as previously described (Northcott et al. 2012. Acta Neuropathol, 123(4):615-26).
Event	DNA copy-number aberration (gain or loss) that spans at least an entire chromosome arm (broad), or a region that is < 12 Mbp in size (focal). G, gains; L, loss.
Identification	Broad and focal copy-number aberrations were identified by Affymetrix SNP6 copy-number profiling as previously described (Northcott et al. 2012. Nature, 488(7409):49-56).
Chromosome-arm	Distinction is made between two types of chromosome-arm events: isolated (P or Q) and non-isolated (p or q). Isolated arm events occur in the absence of whole-chromosome event; non-isolated events may occur in the context of a whole-chromosome event. For example, chr17q|G denotes the gain of chr17q or gain of chr17, whereas chr17Q|G denotes the gain of chr17q without concurrent gain of the whole chr17.
Comparison	For broad cytogenetic markers, the survival of patients whose tumours harbour gain or loss of the indicated chromosome arm were compared against those whose tumours have balanced copy-number for the said chromosome arm. For focal events, patients whose tumours harbour the events were compared against those whose tumours do not harbour the same focal event but may harbour broad events encompassing the locus.
Sample size	Sample sizes required to achieve 80% power in prospective trials are estimated based on the observed hazard ratio. Unbalanced design assumes that the proportion of test group subjects will be equal to the observed frequency of subjects wth the event in the discovery cohort. Balanced design assumes that the test and reference groups will be equal in size.

Appendix Table A8. Analysis of candidate prognostic molecular markers in SHH medulloblastoma for the discovery cohort	
Worksheets	
Description	Description of worksheets.
Log-rank	Significance testing of overall survival differences between patients with or without biomarkers by the log-rank test.
Cross-validation	Cross-validation analyses of prognostically significant biomarkers.
Power	Sample size calculations under Cox proportional-hazards models of candidate prognostic biomarkers for prospective trials.
Definitions	
Survival	Patient overall survival, right-censored at 5 years after diagnosis.
Subgroup	Molecular subgroup of medulloblastoma, determined by a nanoString-based assay as previously described (Northcott et al. 2012. Acta Neuropathol, 123(4):615-26).
Event	DNA copy-number aberration (gain or loss) that spans at least an entire chromosome arm (broad), or a region that is < 12 Mbp in size (focal). G, gains; L, loss.
Identification	Broad and focal copy-number aberrations were identified by Affymetrix SNP6 copy-number profiling as previously described (Northcott et al. 2012. Nature, 488(7409):49-56).
Chromosome-arm	Distinction is made between two types of chromosome-arm events: isolated (P or Q) and non-isolated (p or q). Isolated arm events occur in the absence of whole-chromosome event; non-isolated events may occur in the context of a whole-chromosome event. For example, chr17q|G denotes the gain of chr17q or gain of chr17, whereas chr17Q|G denotes the gain of chr17q without concurrent gain of the whole chr17.
Comparison	For broad cytogenetic markers, the survival of patients whose tumours harbour gain or loss of the indicated chromosome arm were compared against those whose tumours have balanced copy-number for the said chromosome arm. For focal events, patients whose tumours harbour the events were compared against those whose tumours do not harbour the same focal event but may harbour broad events encompassing the locus.
Sample size	Sample sizes required to achieve 80% power in prospective trials are estimated based on the observed hazard ratio. Unbalanced design assumes that the proportion of test group subjects will be equal to the observed frequency of subjects wth the event in the discovery cohort. Balanced design assumes that the test and reference groups will be equal in size.
Worksheets	
Description	Description of worksheets.

Log-rank	Significance testing of overall survival differences between patients with or without biomarkers by the log-rank test.
Cross-validation	Cross-validation analyses of prognostically significant biomarkers.
Power	Sample size calculations under Cox proportional-hazards models of candidate prognostic biomarkers for prospective trials.
Definitions	
Survival	Patient overall survival, right-censored at 5 years after diagnosis.
Subgroup	Molecular subgroup of medulloblastoma, determined by a nanoString-based assay as previously described (Northcott et al. 2012. Acta Neuropathol, 123(4):615-26).
Event	DNA copy-number aberration (gain or loss) that spans at least an entire chromosome arm (broad), or a region that is < 12 Mbp in size (focal). G, gains; L, loss.
Identification	Broad and focal copy-number aberrations were identified by Affymetrix SNP6 copy-number profiling as previously described (Northcott et al. 2012. Nature, 488(7409):49-56).
Chromosome-arm	Distinction is made between two types of chromosome-arm events: isolated (P or Q) and non-isolated (p or q). Isolated arm events occur in the absence of whole-chromosome event; non-isolated events may occur in the context of a whole-chromosome event. For example, chr17q|G denotes the gain of chr17q or gain of chr17, whereas chr17Q|G denotes the gain of chr17q without concurrent gain of the whole chr17.
Comparison	For broad cytogenetic markers, the survival of patients whose tumours harbour gain or loss of the indicated chromosome arm were compared against those whose tumours have balanced copy-number for the said chromosome arm. For focal events, patients whose tumours harbour the events were compared against those whose tumours do not harbour the same focal event but may harbour broad events encompassing the locus.
Sample size	Sample sizes required to achieve 80% power in prospective trials are estimated based on the observed hazard ratio. Unbalanced design assumes that the proportion of test group subjects will be equal to the observed frequency of subjects wth the event in the discovery cohort. Balanced design assumes that the test and reference groups will be equal in size.

Appendix Table A9. Analysis of candidate prognostic molecular markers in Group3 medulloblastoma for the discovery cohort	
Worksheets	
Description	Description of worksheets.
Log-rank	Significance testing of overall survival differences between patients with or without biomarkers by the log-rank test.
Cross-validation	Cross-validation analyses of prognostically significant biomarkers.
Power	Sample size calculations under Cox proportional-hazards models of candidate prognostic biomarkers for prospective trials.
Definitions	
Survival	Patient overall survival, right-censored at 5 years after diagnosis.
Subgroup	Molecular subgroup of medulloblastoma, determined by a nanoString-based assay as previously described (Northcott et al. 2012. Acta Neuropathol, 123(4):615-26).
Event	DNA copy-number aberration (gain or loss) that spans at least an entire chromosome arm (broad), or a region that is < 12 Mbp in size (focal). G, gains; L, loss.
Identification	Broad and focal copy-number aberrations were identified by Affymetrix SNP6 copy-number profiling as previously described (Northcott et al. 2012. Nature, 488(7409):49-56).
Chromosome-arm	Distinction is made between two types of chromosome-arm events: isolated (P or Q) and non-isolated (p or q). Isolated arm events occur in the absence of whole-chromosome event; non-isolated events may occur in the context of a whole-chromosome event. For example, chr17q|G denotes the gain of chr17q or gain of chr17, whereas chr17Q|G denotes the gain of chr17q without concurrent gain of the whole chr17.
Comparison	For broad cytogenetic markers, the survival of patients whose tumours harbour gain or loss of the indicated chromosome arm were compared against those whose tumours have balanced copy-number for the said chromosome arm. For focal events, patients whose tumours harbour the events were compared against those whose tumours do not harbour the same focal event but may harbour broad events encompassing the locus.
Sample size	Sample sizes required to achieve 80% power in prospective trials are estimated based on the observed hazard ratio. Unbalanced design assumes that the proportion of test group subjects will be equal to the observed frequency of subjects wth the event in the discovery cohort. Balanced design assumes that the test and reference groups will be equal in size.

Appendix	**Table A10. Analysis of candidate prognostic molecular markers in Group4 medulloblastoma for the discovery cohort2**
Worksheets	
Description	Description of worksheets.
Log-rank	Significance testing of overall survival differences between patients with or without biomarkers by the log-rank test.
Cross-validation	Cross-validation analyses of prognostically significant biomarkers.
Power	Sample size calculations under Cox proportional-hazards models of candidate prognostic biomarkers for prospective trials.
Definitions	
Survival	Patient overall survival, right-censored at 5 years after diagnosis.
Subgroup	Molecular subgroup of medulloblastoma, determined by a nanoString-based assay as previously described (Northcott et al. 2012. Acta Neuropathol, 123(4):615-26).
Event	DNA copy-number aberration (gain or loss) that spans at least an entire chromosome arm (broad), or a region that is < 12 Mbp in size (focal). G, gains; L, loss.
Identification	Broad and focal copy-number aberrations were identified by Affymetrix SNP6 copy-number profiling as previously described (Northcott et al. 2012. Nature, 488(7409):49-56).
Chromosome-arm	Distinction is made between two types of chromosome-arm events: isolated (P or Q) and non-isolated (p or q). Isolated arm events occur in the absence of whole-chromosome event; non-isolated events may occur in the context of a whole-chromosome event. For example, chr17q|G denotes the gain of chr17q or gain of chr17, whereas chr17Q|G denotes the gain of chr17q without concurrent gain of the whole chr17.
Comparison	For broad cytogenetic markers, the survival of patients whose tumours harbour gain or loss of the indicated chromosome arm were compared against those whose tumours have balanced copy-number for the said chromosome arm. For focal events, patients whose tumours harbour the events were compared against those whose tumours do not harbour the same focal event but may harbour broad events encompassing the locus.
Sample size	Sample sizes required to achieve 80% power in prospective trials are estimated based on the observed hazard ratio. Unbalanced design assumes that the proportion of test group subjects will be equal to the observed frequency of subjects wth the event in the discovery cohort. Balanced design assumes that the test and reference groups will be equal in size.